Archives of Toxicology

The Ca2+-calmodulin-Ca2+/calmodulin-dependent protein kinase II pathway is involved in oxidative stress-induced mitochondrial permeability transition and apoptosis in rat hepatocytes.

--Manuscript Draft--

Manuscript Number:	ATOX-D-14-00006
Full Title:	The Ca2+-calmodulin-Ca2+/calmodulin-dependent protein kinase II pathway is involved in oxidative stress-induced mitochondrial permeability transition and apoptosis in rat hepatocytes.
Article Type:	Original Article
Corresponding Author:	Marcelo G Roma ARGENTINA
Corresponding Author Secondary Information:	
Corresponding Author's Institution:	
Corresponding Author's Secondary Institution:	
First Author:	Flavia D Toledo, grade (biochemistry)
First Author Secondary Information:	
Order of Authors:	Flavia D Toledo, grade (biochemistry)
	Leonardo M Perez, PhD
	Cecilia L Basiglio, PhD
	Enrique J Sánchez Pozzi, PhD
	Marcelo G Roma
Order of Authors Secondary Information:	
Abstract:	Oxidative stress is a common event in most hepatopathies, leading to mitochondrial permeability transition pore (MPTP) formation and further exacerbation of both oxidative stress from mitochondrial origin and cell death. Intracellular Ca2+ elevations play a permissive role in these events, but the underlying mechanisms are poorly known. We examined in primary cultured rat hepatocytes whether the Ca2+/calmodulin (CaM)-dependent protein kinase II (CaMKII) signalling pathway is involved in this process, by using tert-butyl hydroperoxide (tBOOH) as a pro-oxidizing, model compound. tBOOH (500 μM, 15 min) induced MPTP formation, as assessed by measuring mitochondrial membrane depolarization as a surrogate marker, and increased lipid peroxidation in a clyclosporin A (CsA)-sesitive manner, revealing the involvement of MPTPs in tBOOH-induced ROS formation. Intracellular Ca2+ sequestration with BAPTA/AM, CaM blockage with W7 or trifluoperazine, and CaMKII inhibition with KN-62 all fully prevented tBOOH-induced MPTP opening and reduced tBOOH-induced lipid peroxidation to a similar extent to CsA, suggesting that Ca2+/CaM/CaMKII signaling pathway fully mediates MPTP-mediated mitochondrial ROS generation. tBOOH induced apoptosis, as shown by flow cytometry of annexin V/propidium iodide, mitochondrial release of cytochrome c, activation of caspase-3 and increase in the Bax-to-Bcl-xL ratio, and the Ca2+/CaM/CaMKII signaling antagonists fully prevented these effects. Intramitochondrial CaM and CaMKII were partially involved in tBOOH-induced MPTP formation, since W7 and KN-62 both attenuated the tBOOH-induced, MPTP-mediated swelling of isolated mitochondria. We concluded that Ca2+/CaM/CaMKII signaling pathway is a key mediator of oxidative stress-induced induced MPTP formation, and the subsequent exacerbation of oxidative stress from mitochondrial origin and apoptotic cell death.
Suggested Reviewers:	Silvana Zanlungo, PhD

	Associate Professor, , Pontificia Universidad Católica de Chile silvana@med.puc.cl Dr. Zanlungo has been actively working in mechanism involved in oxidative stress in several pathological models, including hepatic ones.
	Juan J Poderoso, PhD Full Professor, University of Buenos Aires jpoderos@fmed.uba.ar Dr. Poderoso is a leading researcher in oxidative stress induced mitochondrial damage and the the involvement of signaling mechanisms.

The Ca^{2+}-calmodulin-Ca^{2+}/calmodulin-dependent protein kinase II pathway is involved in oxidative stress-induced mitochondrial permeability transition and apoptosis in isolated rat hepatocytes

FLAVIA D. TOLEDO[1], LEONARDO M. PÉREZ[1], CECILIA L. BASIGLIO[1],

ENRIQUE J. SANCHEZ POZZI[1] AND MARCELO G. ROMA[1]

[1]*Instituto de Fisiología Experimental, CONICET-Universidad de Rosario, ARGENTINA.*

Author for correspondence:
Dr. Marcelo G. Roma
Instituto de Fisiología Experimental (IFISE)
Facultad de Ciencias Bioquímicas y Farmacéuticas
Suipacha 570, 2000 – Rosario, ARGENTINA
Tel.: +54-341-4305799
Fax: +54-341-4399473
E-mail: mroma@fbioyf.unr.edu.ar

ABSTRACT

Oxidative stress is a common event in most hepatopathies, leading to mitochondrial permeability transition pore (MPTP) formation and further exacerbation of both oxidative stress from mitochondrial origin and cell death. Intracellular Ca^{2+} elevations play a permissive role in these events, but the underlying mechanisms are poorly known. We examined in primary cultured rat hepatocytes whether the Ca^{2+}/calmodulin (CaM)-dependent protein kinase II (CaMKII) signalling pathway is involved in this process, by using *tert*-butyl hydroperoxide (*t*BOOH) as a pro-oxidizing, model compound. *t*BOOH (500 µM, 15 min) induced MPTP formation, as assessed by measuring mitochondrial membrane depolarization as a surrogate marker, and increased lipid peroxidation in a clyclosporin A (CsA)-sesitive manner, revealing the involvement of MPTPs in *t*BOOH-induced ROS formation. Intracellular Ca^{2+} sequestration with BAPTA/AM, CaM blockage with W7 or trifluoperazine, and CaMKII inhibition with KN-62 all fully prevented *t*BOOH-induced MPTP opening and reduced *t*BOOH-induced lipid peroxidation to a similar extent to CsA, suggesting that Ca^{2+}/CaM/CaMKII signaling pathway fully mediates MPTP-mediated mitochondrial ROS generation. *t*BOOH induced apoptosis, as shown by flow cytometry of annexin V/propidium iodide, mitochondrial release of cytochrome *c*, activation of caspase-3 and increase in the Bax-to-Bcl-xL ratio, and the Ca^{2+}/CaM/CaMKII signaling antagonists fully prevented these effects. Intramitochondrial CaM and CaMKII were partially involved in *t*BOOH-induced MPTP formation, since W7 and KN-62 both attenuated the *t*BOOH-induced, MPTP-mediated swelling of isolated mitochondria. We concluded that Ca^{2+}/CaM/CaMKII

signaling pathway is a key mediator of oxidative stress-induced induced MPTP formation, and the subsequent exacerbation of oxidative stress from mitochondrial origin and apoptotic cell death.

Keywords:

Oxidative stress

tert-butyl hydroperoxide

Ca^{2+}/Calmodulin -dependent protein kinase II

Mitochondrial permeability transition pore

Apoptosis

Cytochrome *c*

INTRODUCTION

Radical oxygen species (ROS) occurring under oxidative stress (OS) conditions plays a pivotal role in a wide variety of pathophysiological conditions (Muriel 2009), by oxidizing membrane phospholipids, proteins and nucleic acids (Cochrane 1991). The cellular alterations induced by this redox misbalance depend on the intensity and duration of the oxidative injury. High levels of OS lead predominantly to dramatic changes in plasma membrane permeability, release of cytosolic and mitochondrial components, impaired mitochondrial adenosine triphosphate (ATP) production and, finally, necrosis. Contrarily, lower levels of OS unable to deplete ATP levels cause apoptosis, since apoptosis is an energy-requiring process (Eguchi 1997).

Opening of mitochondrial permeability transition pores (MPTPs) under OS conditions has been implicated as a key, causative event in both manners of cell death. MPTP occurs by the dynamic association of a multiprotein complex of constitutive and regulatory proteins at the sites where the outer mitochondrial membrane is in contact with the inner mitochondrial membrane. The nature of this complex is uncertain, but it may involve a number of putative constitutive proteins such as the voltage dependent anion channel (VDAC) in the outer membrane, adenine nucleotide translocase (ANT), F_0 /F_1 ATP synthase, and the phosphate carrier (PiC) in the inner membrane, and some regulatory proteins, such as cyclophilin D and complement component 1, q subcomponent binding protein (C1QBP), localized in the matrix; fom all of them, only cyclophilin D has held up to genetic scrutiny as an essential protein involved in MPTP formation (Elrod 2013). MPTP opening leads to an abrupt increase in the permeability of the inner mitochondrial

membrane to small molecular weight solutes (< 1500 Da); this collapses ion gradients across the inner mitochondrial membrane, leading to mitochondrial depolarization, uncoupling of oxidative phosphorylation and, eventually, ATP depletion (Jeong 2008; Imberti 1993). MPTP onset also causes mitochondrial swelling, with rupture of the mitochondrial outer membrane and release of cytochrome *c* and other pro-apoptotic molecules from the inter-membrane space to the cytosol (*e.g.*, apoptosis inducing factor, Smac/Diablo). These molecules, together with other cytosolic factors, set off a cascade of caspase activity that leads to apoptotic cell death (Jeong 2008). Alternatively, the release of these proteins may occur through specific changes in the outer membrane permeability, by translocation from cytosol of pro-apoptotic, pore-forming proteins such, as Bax and Bid (Korsmeyer 2000).

Appart from governing cell death, MPTPs aggravates the initial OS that triggers its primary onset. This occurs by (*a*) MPTP-induced loss of cytochrome *c*, which impairs the flow of electrons in the respiratory chain inducing overreduction of the complexes and leakage of electrons to the cytosol, (*b*) reduction of the electron acceptor, NAD^+, which results in ROS emission from the α-ketoglutarate dehydrogenase complex, and (*c*) loss of glutathione from the matrix, which decreases the mitochondrial capacity to scavenge ROS (Chinopoulos 2006).

Another major feature of the oxidative injury is the increase in cytosolic, free Ca^{2+} levels; this activates Ca^{2+}-dependent degradative enzymes, such as phospholipases, proteases and endonucleases, which play a major role in the onset of cell death (Orrenius 1992). In addition, cellular Ca^{2+} elevations exacerbates OS-induced cell death (Thor 1984), by potentiating the capability of ROS to onset MPTP opening (Byrne 1999). Some

hypotheses have been advanced to explain this fact, although any of them have been proved conclusively as yet. OS causes release of matrix Ca^{2+} that can be taken up back into the mitochondria (Ca^{2+} cycling); this excessive Ca^{2+} cycling has been proposed to be responsible for MPTP onset (Takeyama 1993). In addition, elevations of mitochondrial matrix free Ca^{2+} may increase mitochondrial respiration, which is controlled by Ca^{2+}-regulated mitochondrial dehydrogenases. This latter process may overstimulate mitochondrial ROS production, thus triggering MPTP by oxidation of free thiol groups in ANT, which increases the affinity of this protein for cyclophilin D to induce MPTP generation (Kanno 2004). In addition, OS greatly enhances MPTP sensitivity to Ca^{2+}. This occurs both by increasing cyclophilin D binding to ANT, a critical step in MPTP formation, and by reducing the affinity of the intramitochondrial adenine nucleotide-binding site on ANT; the binding of adenine nucleotides to this site inhibits competitively Ca^{2+}-dependent MPTP formation (Halestrap 2000). Therefore, cellular Ca^{2+} overload occurring under OS conditions would represent a vicious circle by which Ca^{2+} and ROS mutually potentiate each other to exacerbate ROS formation from mitochondrial origin, which induces further Ca^{2+} increments.

Although there is compelling evidence in the literature that Ca^{2+} is involved in ROS-induced-MPTP opening in hepatocytes, there is no agreement as yet on the mechanisms underlying this effect. A likely candidate to mediate Ca^{2+}-dependent mitochondrial damage is calmodulin (CaM). This protein binds Ca^{2+}, and the complex is involved in a variety of cell functions through the activation of CaM-dependent enzymes (Colbran 2004). CaM is an ubiquitous protein found mainly in liver cytoplasm, nucleus, and plasma membrane (Harper 1980), but mitochondria also contain CaM both on the inner membrane and in the matrix space (Itano 1986). The organelle holds several CaM-binding proteins as well,

which have been implied as mediators of mitochondrial permeability transition (MPT) and cell death. They include the phosphatase calcineurin (Molkentin 2001), the cysteine protease calpain (Arrington 2006), and protein quinase Ca^{2+}/calmodulin-dependent protein kinase II (CaMKII) (Joiner 2012). Therefore, at least conceptually, Ca^{2+} overload occurring under OS-conditions may excessively activate these CaM-downstream targets, leading to MPTP opening and mitochondrial ROS generation.

In this work, we addressed this hypothesis by using *tert*-butyl hydroperoxide (*t*BOOH) as a pro-oxidant compound. *t*BOOH is a synthetic analogue of short-chain lipid hydroperoxides formed endogenously under OS conditions, which has been widely used as a model to study the effect of OS on biological systems (Nieminen 1995; Byrne 1999; Imberti 1993). Apart from inducing OS directly via reduction into both peroxyl and alkoxyl free radicals by both cytochrome P450 and the mitochondrial electron chain (Davies 1989), *t*BOOH promotes OS via ROS-induced MPTP formation and further mitochondrial production of ROS. This is supported by the finding that MPTP blockers inhibit the late phase of mitochondrial pyridine-nucleotide oxidation and ROS generation following *t*BOOH exposure to isolated hepatocytes (Nieminen 1997). This makes *t*BOOH a unique tool to study the factors regulating OS-dependent MPTP onset, and the further hepatocellular death.

MATERIAL AND METHODS

Materials. Collagenase type A from Clostridium histolyticum was purchased from Gibco (Paisley, UK). Leibovitz-15 (L-15) tissue culture medium, bovine serum albumin (fraction V), *t*BOOH, dimethylsulphoxyde (DMSO), Triton X-100, EGTA, sodium dodecyl sulfate (SDS), TEMED, DTT , leupeptin, urethane, PMSF, cyclosporin A (CsA), trifluorperazine (TFP), FK-506 (tacrolimus), carbonyl cyanide m-chloro-phenylhydrazone (CCCP) and tetramethylrhodamine methyl ester (TMRM) were from Sigma Chemical Co. (St. Louis, MO). Cellular lysis buffer, KN-62, W7, mouse anti-CaMKII, and mouse anti rat phospho-CaMKII were from Cell Signaling Technology (Beverly, MA). BAPTA/AM and Fura-2/AM were from Molecular Probes (Eugene, Oregon, U.S.A.). Goat anti-mouse IgG (#31430), chemiluminescence reagent, and Hyperfilm ECL were from Thermo Fisher Scientific Inc. (Waltham, MA). All other chemicals were of reagent grade.

Animals. Adult male Wistar rats weighing 300-350 g were used throughout. Animals were maintained on a standard diet and water ad libitum, and housed in a temperature (21º-23º C) and humidity (45-50%) controlled room, under a constant 12-hour light, 12-hour dark cycle. All animals received humane care, according to the Guide for the Care and Use of Laboratory Animals prepared by the National Academy of Sciences and published by the NIH (publication 25-28, revised 1996).

Hepatocyte isolation. Hepatocytes were isolated from livers by the collagenase perfusion

technique, using a modification of the method of Berry and Friend (Berry 1969). Briefly, under urethane anesthesia (5mg/kg body wt, ip), heparin was administered in the inferior vena cava (1.50 U/kg of body weight), and a 14G catheter (Abbocath-T, Venisystemtm, Abbocath Ireland Ltd., Sligo, Ireland) was introduced in the portal vein. This was followed by a 10-min, non-recirculant portal perfusion with a Ca^{2+}-free, oxygenated (95% O2/5% CO2) Hanks' solution, pH = 7.47-7.50, supplemented with HEPES (3 g/l) and EGTA (0.24 g/l). The livers were then perfused for a further 5-min period with the same solution without EGTA, supplemented with 1 mM $MgSO_4$, 2.5 mM $CaCl_2$ and collagenase type IV (430 U/l). Finally, the livers were removed, and the cells isolated by mechanical dissociation by gently stirring with a glass stick for 3-4 min. Hepatocytes were further purified from non-parenchymal cells by low-speed centrifugation (30xg, 2 min), followed by 3 consecutive washings in oxygenated Hanks' solution containing 2.5 mM $CaCl_2$ and 5 mM Tris. The resulting preparation yielded ~ 400-600x10^6 hepatocytes per liver, with high viability (>90%), as assessed by the trypan blue exclusion test (Baur 1975).

Hepatocyte culture. Isolated hepatocytes were plated in 6-well plastic plates precoated with rat tail collagen at least 1 day before preparing the hepatocyte cultures. Ice-cold neutralized collagen solution was dispensed onto each dish/well, and the coated dishes/plates were placed at 37º C in a humidified incubator for approximately 2 h to allow the matrix material to gel, followed by addition of 3 ml of DMEM to each dish/plate and storage in a humidified incubator. Hepatocyte suspensions were added to the precoated dishes/plates at a density of 2 x 10^6 cells/ 30mm dishes diluted in DMEM. Cells were allowed to attach for 2-2.5 h at 37º C in a air humidified atmosphere and 5 % CO2. After attachment, the

medium was aspirated, and 3 ml of fresh DMEM was added.

Treatments. After 18 h of culture, hepatocytes were incubated with 500 µM *t*BOOH (or the vehicle, DMSO, in controls) for 15 min in a humidified incubator at 37º C, with 5% CO_2. The effect of the pre-incubation of the hepatocytes with a number of modulators was studied. Hepatocytes were pre-incubated with these modulators for 15 min, and then exposed to *t*BOOH for a further 15-min period. The modulators were kept in the incubation medium throughout *t*BOOH exposure.

Evaluation of tBOOH effect on hepatocellular integrity. At the end of the incubation period with *t*BOOH, aliquots of hepatocytes were removed to assess cell viability, leakage of the cytosolic enzyme, lactate dehydrogenase (LDH; EC 1.1.1.27), and ATP content.

Viability of hepatocytes cultured on multiwell plates was assessed by the trypan blue exclusion test (Baur 1975).

Plasma membrane integrity was evaluated by the leakage of the cytosolic enzyme, LDH, into the incubation medium. LDH activity was assessed spectrophotometrically (Perkin Elmer UV/Vis Spectrometer Lambda2S, berlingen, Germany) by measuring NADH consumption at 340 nm, using commercial kits (LDH-P UV AA liq, Wiener Lab., Rosario, Argentina). LDH release (activity in the medium) was normalized to total LDH activity in the cellular compartment. For this purpose, aliquots of the cellular suspension were treated with Triton X-100 (0.1% v/v), followed by centrifugation at 9000xg for 2 min.

ATP content was measured using the substrate-enzyme system, luciferin-luciferase

(Lyman 1967).

Evaluation of tBOOH-induced OS. The magnitude of OS induced by *t*BOOH was evaluated in hepatocytes cultured in precoated dishes by measuring generation of the lipid peroxidation product malondialdehyde (MDA), and the oxidized glutathione (GSSG)-to-total glutathione (GSHt) ratio.

MDA was measured by reaction with thiobarbituric acid followed by the fluorimetrical HPLC detection of the MDA-thiobarbituric acid adduct formed, according to the HPLC method of Fukunaga *et al.* (Fukunaga 1998). A standard curve using 1,1,3,3-tetramethoxypropane, which is converted mol for mol into MDA, was routinely run.

Cell contents of GSHt and GSSG were determined by the recycling method of Tietze (Tietze 1969), as modified by Griffith (Griffith 1980).

Protein content in the aliquots of cell suspension used for the assay was measured by the method of Lowry *et al.* (Lowry 1951), using BSA as a standard.

Measurement of cytosolic Ca^{2+} concentration ($[Ca^{2+}]_i$). $[Ca^{2+}]_i$ was assessed using Fura-2/AM as a probe. For this purpose, 2 x 10^6 cells were suspended at 37º C in 3 ml of a PBS (pH = 7.4) buffer solution containing 3 mM $CaCl_2$, and then supplemented with 1µM Fura-2/AM. Fluorescence intensity (F) was measured by using alternating excitation wavelengths of 340 and 380 nm, and a fluorescence emission wavelength of 510 nm (3 nm bandwidth). $[Ca^{2+}]_i$ was calculated from the 340 nm/380 nm Fura-2/AM fluorescence intensity ratio (R), according to the following equation (Grynkiewicz 1985):

$$[Ca^{2+}]_i = K_d\,[(R-R_{min})/(R_{max}-R)]\,(F380_{min}/F380_{max})$$

where K_d is the dissociation constant of the complex Fura-2/Ca^{2+} (135 nM), R_{max} and R_{min} are R values measured sequentially by addition of 10g/ml digitonin to the Fura-2-loaded cells before and after chelating Ca^{2+} with 5 mM EGTA/Tris solution (pH = 8.7), respectively.

Assessment of MPTP formation. MPTP generation was evaluated in primary culture of rat hepatocytes by assessing the mitochondrial membrane potential as a surrogate marker, using TMRM as a probe (Imberti 1993); TMRM is a membrane-permeable, cationic fluorophore that accumulates electrophoretically in mitochondria in proportion to their membrane potential ($\Delta\psi$). For this purpose, hepatocytes in 24-well plates were loaded at 37º C with 8 µM TMRM in Krebs-Henseleit buffer for 10 min. The supernatant was then aspirated to remove the excess of TMRM, and fluorescence intensity was measured using a fluorescence multiwell plate reader using excitation and emission filters of 546 and 573 nm, respectively. Mitochondrial $\Delta\psi$ was calculated from the 573 nm/546 nm TMRM fluorescence intensity ratio (R), according to Scaduto and Grotyohann (Scaduto, Jr. 1999), and expressed as the percentage of the change in mitochondrial depolarization, in a scale ranging from a basal, non-depolarized condition (control value) to the maximal depolarized condition, obtained by adding the respiratory chain uncoupling compound, CCCP (10 µM).

Additionally, MPT was assessed in isolated mitochondria by monitoring the changes in mitochondrial osmotic volume (swelling) secondary to MPTP formation. Swelling was monitored by the decrease in apparent absorbance (light-scattering), since the light scattered is inversely proportional to the mitochondrial volume (Azzone 1965). For this

purpose, the mitochondrial fraction (1 mg protein/ml) was resuspended in 1 ml of swelling buffer composed of 5 mM KH_2PO_4, 200 mM sucrose, 5 mM succinate (for mitochondria energization), and 25 mM KCl (pH = 7.4). After a 2-min equilibration period, *t*BOOH (or its vehicle, saline) was added so as reach a final concentration of 500 μM, and swelling was monitored by recording the changes in absorbance at 540 nm with a Perkin Elmer Lambda 2S UV-Vis spectrophotometer computer controlled (Norwalk, USA).

Analysis of protein kinase activation. The activation of CaMKII and mitogen-activated protein kinases (MAPKs) of the c-Jun NH2-terminal kinase 1/2 (JNK1/2) and $p38^{MAPK}$ types were assessed by Western blotting using a antibodies recognizing the activate forms of these kinases, which are phosphorylated at Thr^{286}, Thr^{183}/Tyr185, and Thr^{180}/Tyr^{182}, respectively.

For this purpose, the content of phosphorylated and total forms of the proteins was analyzed by Western blotting of primary hepatocyte cultures. After treatment, hepatocytes were washed with cold PBS and resuspended in a cellular lysis buffer containing protease inhibitors (leupeptin 25 g/ml and PMSF 0.1 mM). Aliquots containing equivalent total protein content were subjected to SDS, 12% polyacrylamide gel electrophoresis. Separated proteins were electrotransferred to PVDF membranes, and probed overnight with anti-phospho-CaMKII (1:2000), anti-phospho-JNK1/2 antibody (1:2000), or anti-phospho-$p38^{MAPK}$ (1:300) antibodies. Membranes were then stripped, and reproved with an anti total-CaMKII (1:2000), anti–total JNK1/2 (1:5000), or anti-total $p38^{MAPK}$ (1:500) antibodies. After using a goat anti-mouse or a mouse anti-goat IgG secondary antibody (1:5000) depending on the primary antibody used, a chemiluminescence reagent, and Hyperfilm

ECL, the phospho and total bands of each studied protein were quantified by densitometry using the Image J 1.34m software.

Apoptosis analysis. Apoptosis was evaluated by the Annexin V/ propidium iodide (PI) flow cytometry assay (Vermes 1995). In addition, the involvement of the mitochondrial apoptosis pathway in *t*BOOH-induced hepatocellular death was studied by assessing mitochondrial cytochrome *c* release into cytosol, the subsequent increase in caspase-3 activity, and the balance between proapoptotic (Bax) and antiapoptotic (Bcl-xL) mitochondrial proteins.

Annexin V flow cytometry assay. After gently homogenization in the culture medium/PBS and harvest (5 min, 400 g), hepatocytes were carefully re-suspended in the appropriate buffer at the desired concentration. Apoptotic externalization of phosphatidylserine and cell death in hepatocytes was assessed by staining with Annexin V-FITC and PI (Annexin V-FITC Apoptosis Detection Kit, Sigma Chemical Co, St Louis, MO), respectively, coupled to flow cytometric analysis (Cell Sorter BD FACSAria II, Becton, Dickinson and Co, Franklin Lakes, NJ), following the manufacturer's instructions. Detection of green and red fluorescence was carried out; green and red fluorescence intensities detected in non stained cells were used to set the thresholds for each channel. Annexin V positive cells, irrespective of whether they were PI positive or negative cells, were considered to be apoptotic in nature, either at an early stage of apoptosis (annexin V positive/PI negative cells) or at an late stage of apoptosis (annexin V positive/PI positive cells). Even when necrotic cells all share the same features as late stage apoptotic cells in terms of pattern of annexin V/propidium iodide staining, necrosis can be ruled out from our results showing conserved

ATP cellular content (Table 1). Indeed, for the occurrence of apoptosis, normal levels of ATP are necessary, whereas low cellular ATP levels are indicative of necrosis (Eguchi 1997).

Immunoblot analysis of pro- and anti-apoptotic proteins. The levels of cytochrome *c* (in cytosol) and of Bax and Bcl-xL (mitochondria), all proteins involved in the apoptosis process, was determined by immunoblotting. Cytosolic and mitochondrial fractions were prepared by differential centrifugation, as previously described (Kim 2006). Briefly, mitochondria-enriched fractions were prepared from hepatocytes that were homogenized in sacarose 0.3 M with protease inhibitors (1 mM phenylmethylsulfonyl fluoride, 10 mg/ml leupeptin, and 1 mg/ml aprotinin), and sonicated. Homogenates were centrifuged at 1000xg to remove unbroken cells, nuclei, and heavy membranes. Mitochondria enriched fractions were then obtained by the centrifugation of supernatant at 6000xg at 4°C for 15 min. Then, the supernatant was centrifuged at 45000xg for 1 h to obtain the cytosolic fraction (Ronco 2004). Proteins were quantified in these fractions according to Lowry *et al.* (LOWRY 1951). For immunoblotting, 20 µg of protein were subjected to 12% SDS-PAGE, and transferred to Immobilon polyvinylidene difluoride (PVDF) membranes (Perkin Elmer Life Sciences, Boston, MA, USA). Membranes were blocked with 5% non-fat milk/0.3% Tween/PBS, washed, and incubated overnight at 4 ºC with a specific primary antibody against Bax, Bcl-xL, or cytochrome *c* (1:600, Santa Cruz Biotechnology, Santa Cruz, CA, USA). Then, membranes were incubated with the appropriate secondary antibody conjugated with horseradish peroxidase (1:5000, Amersham Life Science), and the resulting bands were detected by enhanced chemiluminescence (ECL; Amersham Pharmacia Biotech). Autoradiographs were obtained by exposing PVDF membranes to

Amersham hyperfilmTM ECL (GE Healthcare), and the bands quantified by densitometry using the Gel-Pro Analyzer software (Media Cybernetics, Silver Spring, MD).

Assessment of caspase-3 activity. Caspase-3 activity was determined according to the manufacturer's instructions, using an EnzChek caspase-3 assay kit (Molecular Probes, Eugene, OR, USA). The tissues were homogenized in lysis buffer (10 mM Tris, 200 mM NaCl, 1 mM EDTA, and 0.001% Triton X-100). After differential centrifugation, the cytosolic fraction from each sample was mixed with a Z-Asp-Glu-Val-Asp-AMC substrate solution. A standard curve of AMC ranging from 0-100 mM was run. A control sample without enzyme was used to determine the background fluorescence of the substrate. Fluorescence was measured at an excitation wavelength of 360 nm and an emission wavelength of 465 nm in a DTX 880 Multimode Detector (Beckman Coulter, Brea, CA, USA).

Statistical analysis. Data are expressed as mean ± SE. Multiple means were compared with one-way ANOVA followed by Tukey´s test for pairwise comparisons, by using a computer program (PHARM/PCS, MicroComputer Specialist, Philadelphia). Differences were considered significant when the p values were < 0.05.

RESULTS

Characterization of tBOOH-induced impairment in hepatocellular integrity, oxidative stress generation, changes in ATP content and cytosolic Ca^{2+} elevations. As shown in Table 1, *t*BOOH (500 µM, 15 min) impaired hepatocellular integrity, as indicated by a 38% decrease in cell viability, and a 31% increase in the release to the incubation medium of the cytosolic enzyme, LDH. Contrarily, ATP content was not affected by the oxidant agent.

An increase in ROS levels was clearly apparent after *t*BOOH exposure, as indicated by the enhancement of one order of magnitude in the generation of the lipid peroxide malondialdehyde (Table 1); this was associated with a decrease in both total (GSH + GSSG) glutathione and the GSSG-to-total glutathione ratio. This OS was instrumental in increasing dramatically (by ~25 times) the cytosolic, free Ca^{2+} concentration.

Effect of intracellular Ca^{2+} sequestration and CaM/CaMKII inhibition on tBOOH-induced changes in mitochondrial $\Delta\psi$ and lipid peroxidation (LPO). MPTP formation induced by *t*BOOH was assessed by measuring depolarization of mitochondrial $\Delta\psi$ as a surrogate parameter, using the mitochondrial-sensitive cation TMRM as a probe. The dependency of mitochondrial $\Delta\psi$ on MPTP formation was corroborated by our own result that the MPTP blocker CsA diminished significantly the changes in mitochondrial $\Delta\psi$ induced by *t*BOOH (Fig. 1, *A*); the difference between the changes in mitochondrial $\Delta\psi$ induced by *t*BOOH and the changes of this parameter in the presence of CsA can be thus regarded as a measure of MPTP formation.

The degree of LPO, as measured by MDA content, was dramatically increased by *t*BOOH, and the MPTP blocker CsA inhibited partially this effect (Fig. 1, *B*); a similar phenomenon had been reported elsewhere using the OS-sensitive fluorescent dye dichlorofluorescein as a probe to assess ROS generation (Nieminen 1997). This support the contention that *t*BOOH capability to induce ROS depends not only on the generation of peroxyl- and alkoxyl-free radicals after metabolization (Davies 1989) but also on its capability to induce MPTP formation. This CsA-sensitive fraction of *t*BOOH-induced LPO provides an observational window where the influence of signaling modulators on OS from mitochondrial origin can be monitored.

As can be also seen in Fig. 1 *A* and *B*, the intracellular Ca^{2+}-sequestering agent BAPTA/AM attenuated *t*BOOH-induced both mitochondrial depolarization and LPO to a similar extent to CsA. Overall, these results indicate that *t*BOOH-induced LPO depends partially on MPTP generation, and that this effect is facilitated by intracellular Ca^{2+} elevations.

In an attempt to find it out possible mediators of the facilitating effect of Ca^{2+} on MPTP formation and the further generation of mitochondrial ROS, we assessed the involvement of CaM and two of its putative downstream mediators, CaMKII and calcineurin, in the capability of *t*BOOH to induce MPT and LPO of mitochondrial origin. As shown in Fig. 1 *A* and *B*, respectively, the CaM antagonists TFP and W7 prevented completely the CsA-sensitive changes in mitochondrial $\Delta\psi$ and MDA content induced by *t*BOOH; CsA effect was not additive with that of W7, strongly suggesting that both the MPTP blocker and the CaM inhibitor acts via a similar mechanism, *i.e.* inhibition of MPTP formation. Similarly to the CaM inhibitors, the specific CaMKII inhibitor KN-62, but not

the calcineurin inhibitor FK-506 (tacrolimus), fully prevented both alterations. This indicates that both the onset of MPTP induced by *t*BOOH and the resulting oxidative stress from mitochondrial origin are modulated by CaM, via CaMKII activation.

Effect of tBOOH on CaMKII activation. Western blot analysis of phosphorylated CaMKII showed that the amount of the phosphorylated, active form of CaMKII significantly increased at 15 min after *t*BOOH administration (Fig. 2). On the other hand, total CaMKII content remained unchanged. Pretreatment with the CaM inhibitors TFP and W7, or with the CaMKII inhibitor KN-62, completely prevented the increase in phosphorylated CaMKII. This rules out the alternative possibility that CaMKII is activated by direct oxidation of paired methionine residues in the regulatory domain of CaMKII in the absence of Ca^{2+}/CaM, as was shown to occur in cardiomyocytes (Erickson 2008).

Effect of tBOOH on JNK1/2 and p38^{MAPK} activation. Western blot analysis of phosphorylated and total forms of JNK1/2 and p38 MAPK showed that the amount of the phosphorylated, active form of these MAPKs significantly increased at 15 min of *t*BOOH administration, whereas total JNK1/2 and p38^{MAPK} content remained unchanged (Fig. 3). Pretreatment with the Ca^{2+}-chelating agent BAPTA/AM, the CaM inhibitors TFP and W7, or with the CaMKII inhibitor KN-62 completely prevented the increase in phosphorylated JNK1/2 and p38^{MAPK}.

tBOOH induces apoptosis via the Ca^{2+}/CaM/CaMKII signaling pathway. Because dissipation of the mitochondrial potential is a common and early feature of apoptosis, we

analyzed here whether *t*BOOH exposure leads to apoptosis, and whether inhibition of the Ca^{2+}/CaM/CaMKII signaling pathway at different steps prevents this effect. Cytometric annexin V/propidium iodide assay showed that *t*BOOH significantly increased annexin V (+) /propidium iodide (-) cells (early apoptosis) by 86% (Fig. 4, *A*). The proportion of annexin V (+)/propidium iodide (+) (late apoptosis) also was increased by 122% (Fig. 4, *B*). As a consequence, the proportion of cells with either early or late apoptosis, *i.e.*, annexin V (+) cells, was increased by 89% by *t*BOOH (Fig. 5, *C*). On the other hand, in cell pretreated with inhibitors acting at different levels in the Ca^{2+}/CaM/CaMKII signaling pathway, the proportion of cells with either early apoptosis or late apoptosis after *t*BOOH exposure was similar to that of control cells, or to that treated with the MPTP blocker CsA (Fig. 4, *A* and *B*, respectively). A similar pattern of prevention was obtained when the proportion of apoptotic cells irrespective of their stage was considered (Fig. 4, *C*).

Involvement of the mitochondrial pathway in tBOOH-induced apoptosis. The role for mitochondria in *t*BOOH-induced apoptosis via the Ca^{2+}/CaM/CaMKII signaling pathway was assessed by studying the release of mitochondrial cytochrome *c* into cytosol, the further increase in the activity of caspase-3, and the balance between the mitochondrial pro-apoptotic protein Bax and the anti-apoptotic protein Bcl-xL.

Immunoblot analysis of cytosolic cytochrome *c* showed that there was an increase of ~120% in cytochrome *c* release from mitochondria after *t*BOOH exposure, and that Ca^{2+} sequestration with BAPTA, inhibition of CaM with TFP or W7, and CaMKII inhibition with KN-62 all fully prevented mitochondrial cytochrome *c* release (Fig. 5).

As anticipated from the fact that cytosolic cytochrome *c* triggers apoptosis via

activation of the executioner caspase-3, the activity of this caspase increased aprox. 3 times in cytosol after *t*BOOH exposure. This effect was also fully prevented by the MPTP blocker CsA, indicating that the "intrinsic" (mitochondrion-driven) pathway of caspase-3 activation is triggered by *t*BOOH (Fig. 6). Ca^{2+} sequestration with BAPTA, inhibition of CaM with TFP or W7, and CaMKII inhibition with KN-62 all fully prevented the increase in caspase-3 activity at the same extent as CsA did.

Finally, we examined the expression of Bax and Bcl-xL at the protein level in the mitochondrial fraction by western blot analysis. Bax and Bcl-xL are members of the Bcl-2 family which plays major, opposite roles as regulators of the apoptotic process: while Bax acts as a promoter, Bcl-xL acts as an inhibitor (Tzung 1997). Immunoblot analyses revealed that mitochondrial Bax protein levels increased by 139% ($P < 0.01$) after *t*BOOH administration, whereas Bcl-xL remained virtually unchanged (Fig. 7, *upper panel*). Consequently, Bax-to-Bcl-xL ratio, an indicator of cell vulnerability to apoptosis, was increased by 186% by *t*BOOH (Fig. 7, *lower panel*). Inhibition of CaM with TFP or W7, and inhibition of CaMKII with KN-62 both prevented the increase in both Bax mitochondrial level and Bax-to-Bcl-xL ratio.

Involvement of mitochondrial CaMKII in tBOOH-induced MPTP. CaMKII is a ubiquitous enzyme, and CaMKII with mitochondrial localization has been recently reported to play a crucial role in Ca^{2+}-induced MPTP and apoptosis in cardiomyocytes (Joiner 2012). To assess the involvement of mitochondrion-localized CaMKII in *t*BOOH-induced MPTP formation in hepatocytes, we studied in isolated hepatocellular mitochondria the effect CaMKII on *t*BOOH-induced osmotic swelling of the mitochondrial matrix, a

phenomenon due to opening of MPTPs in the inner mitochondrial membrane. The time course of mitochondrial swelling, as monitored by recording the decrease in absorbance (light-scattering) at 540 nm over 15 min, is shown in Fig. 8. Control mitochondria treated with the *t*BOOH vehicle showed a slight decrease due to spontaneous swelling, whose magnitude agrees with results obtained by others (Roy 2009; Lee 2008). On the other hand, *t*BOOH induced a fast decrease in light scattering due to MPTP formation, as confirmed by the fact that the MPTP blocker CsA fully abrogated this effect. Swelling was less pronounced when either the CaM inhibitor W7 or the CaMKII inhibitor KN-62 was present in the medium, suggesting a partial role for a mitochondrial Ca^{2+}/CaM/CaMKII signalling pathway in *t*BOOH-mediated effect.

DISCUSSION

MPTP onset has been implicated as a pivotal event contributing to hepatocyte cell death under OS conditions. This was readily apparent from studies showing that MPTP blockers inhibit the late phase of mitochondrial pyridine nucleotide oxidation and ROS generation in isolated hepatocytes exposed to *t*BOOH (Nieminen 1997). The MPTPs generated by an initial oxidant insult (ROS generated from *t*BOOH metabolization, in our case) further exacerbate ROS production by inducing leakage of electrons from the mitochondrial respiratory chain, which triggers a detrimental vicious circle (Nieminen 1995).

Despite there is compelling evidence in the literature that Ca^{2+} is involved in MPTP onset caused by oxidizing agents in hepatocytes (Imberti 1993; Byrne 1999), the intracellular events mediating this effect has not been fully clarified as yet; its elucidation is however relevant to develop new therapeutic approaches for protection against OS-induced hepatocellular damage. In this report, we provide novel evidence that the Ca^{2+}/CaM/CaMKII signaling pathway plays a pivotal role in both *t*BOOH-induced MPTP formation in hepatocytes and its potential to exacerbate OS from mitochondiral origin, two events that are linked causally with each other. This is supported by our finding that Ca^{2+} sequestration with BAPTA, blockage of the formation of the Ca^{2+}/CaM complex with W7 or TFP, or inhibition of CaMKII with KN-62 all prevented *t*BOOH-induced OS and MPTP formation to a similar extent to the MPTP blocker CsA (see Fig. 1). Our finding that no additive effect was recorded when both MPTP and CaM were simultaneously inhibited by CsA and W7, respectively (see Fig. 1), further confirms the involvement of MPTP as a common target of both inhibitors.

Disruption of intracellular Ca^{2+} homeostasis and defects in mitochondrial function induce cell death in a variety of pathological conditions involving Ca^{2+} elevations and oxidative damage [for reviews, see (Orrenius 1992; Lemasters 2009)]. Several lines of evidence indicate that many of these detrimental effects are mediated by CaM and/or CaMKII. For example, CaM and CaMKII inhibitors protect against both hypoxia/hypoglycemia- (Hajimohammadreza 1995) and veratridine-induced neuronal depolarization (Takano 2003). In addition, CaM antagonists attenuate MPTP-mediated neuronal death due to ischemia (Kuroda 1997), and apoptotic death of pheochromocytoma cells (PC12) induced by the depolarizing agent 1-methyl-4-phenylpyridinium (Lee 2005). In the latter cell line, ROS formation, cytochrome *c* release, activation of caspase-3 and cell death induced by rotenone, an inhibitor of mitochondrial-respiratory-chain-complex I, was counteracted by CaM antagonists. Similarly, CaM antagonists protected rat heart myocardium H9c2 cells against toxicity of rotenone by suppressing ROS formation (Yaglom 2003). Moreover, in rat ventricular, permeabilized cardiomyocytes, direct CaM exposure induced depolarization of $\Delta\psi$ mitochondrial and opening of MPTP by increasing ROS production in a CaMKII-dependent manner (Odagiri 2009) Finally, CaMKII has been implied in cadmiun-induced apoptosis in mesangial cells (Liu 2007).

The role of Ca^{2+}/CaM/CaMKII signaling pathway in MPTP opening and the associated generation of OS from mitochondrial origin had not been assessed in hepatocytes. Only some reports provides circumstantial evidence that CaM and/or CaMKII are involved in ROS generation and OS-induced liver damage, such as that induced by the hepatotoxicants acetaminophen (Dimova 1995) and CCl_4 (Villarruel 1990). However, the action mechanisms of these toxic compounds are multifactorial in nature, and this prevents

a clear conclusion to be drawn on the CaM and/or CaMKII mechanisms of action. In this work, we provide mechanistic support for these preliminary results by showing that CaM modulates OS from mitochondrial origin via MPTP formation and further apoptotic hepatocellular death, and that this effect involves CaMKII as a main downstream effector.

CaMKII belongs to the multifunctional, Ca^{2+}/CaM-activated, serine/threonine kinase family (Hudmon 2002). Therefore, CaMKII may influence MPTP onset by modifying the phosphorylation status of mitochondrial proteins belonging to, or regulating, MPTP. In line with this, changes in the phosphorylation status of several low-molecular-weight, mitochondrial proteins were observed in rat brain associated with MPTP opening. Interestingly, this phenomenon was dependent on Ca^{2+}, and prevented by the CaM antagonist calmidazolium (Azarashvili 2003).

It is difficult at this stage to identify specific putative structural or regulatory components of the MPTP as target for CaMKII-mediated phosphorylation. To the best of our knowledge, only VDAC has been described to be regulated by different kinases, such as PKA (Bera 2001) and PKCε (Baines 2003), but all these phosphorylations inhibited rather than enhanced MPTP opening probability. Finally, the "novel" PKC isoform PKCδ travels to mitochondria under OS conditions, where it triggers the release of cytochrome *c* and apoptosis (Horbinski 2005; Majumder 2001). However, this member of the "novel" PKC family is unresponsive to Ca^{2+}. Alternatively, the "conventional", Ca^{2+}-dependent PKC isoform PKCα, which we had showed to be activated by *t*BOOH in a previous work even at lower concentrations (100 μM) (Perez 2006), has prosurvival rather than proapoptotic functions in several cell lines (Horbinski 2005; Ruvolo 1998). Lack of involvement of all these PKC isoforms was further confirmed by our results that neither

phorbol-12-myristate 13-acetate nor staurosporine, which activates and inhibits both "conventional" and "novel" PKC isoforms, respectively (Gschwendt 1996), modified *t*BOOH capability to induce ROS generation, MPTP onset and apoptosis (data not shown).

Rather, our results are more consistent with the existence of signaling cascades downstream of CaMKII involving JNK and $p38^{MAPK}$ (see Fig. 3). This finding is in line with previous results showing that CaMKII can phosphorylate and activate both $p38^{MAPK}$ (Nguyen 2004) and JNK1/2 (Brnjic 2010), and that this event leads to apoptosis via activation of the upstream protein *apoptosis signal-regulating kinase 1* (ASK1) (Brnjic 2010; Liu 2013). A rol for these MAPKs in *t*BOOH-induced MPTP opening by phosphorylating apoptosis-related mitochondrial proteins is indeed likely. $p38^{MAPK}$ phosphorylates VDAC in myocardiocytes after myocardial isquemia reperfusion, and the kinase inhibition counteracted necrosis induced by this manoeuvre (Schwertz 2007); unfortunately, MPTP generation was not assessed under this condition. As for JNK, its activation has been shown to trigger Bax translocation to mitochondria by phosphorylation of the Bax cytosolic anchor protein 14-3-3 (Tsuruta 2004); this may explain our finding that mitochondrial Bax content increases after *t*BOOH exposure in a Ca^{2+}/CaM/CaMKII-dependent manner (see Fig. 7). Once in mitochondria, Bax oligomerizes in the outer mitochondrial membrane to form pores, which allows for cytochrome *c* release and further caspase-3 activation (Orrenius 2007), two events that have been also shown to occur here after *t*BOOH exposure in a Ca^{2+}/CaM/CaMKII-dependent manner (see Figs. 5 and 6, respectively). The alternative possibility that JNK regulates Bax by direct phosphorylation is also likely. In the human hepatoma cell line HepG2, various cell death agonists, including pro-oxidant ones, induced apoptosis by promoting mitochondrial Bax

translocation via its phosphorylation at Thr^{167} by both JNK and $p38^{MAPK}$ (Kim 2006). Whether activation of these kinases explains the dependency of *t*BOOH-induced apoptosis on CaMKII activity remains to be ascertained, and this is the subject of ongoing research. The possibility is likely, since CaMKII-dependent activation of JNK has been demonstrated to occur in other cellular models leading to mitochondrion-driven apoptosis (Timmins 2009; Li 2012).

Alternatively, CaMKII may upregulate by phosphorylation the activity of a phosphatase able to activate by dephosphorylation the effects of pro-apoptotic proteins known to be inhibited the phosphorylating activity of other protein kinases. For example, calcineurin, a Ca^{2+}/CaM-dependent, serine-threonine phosphatase, induces apoptosis by promoting Bad dephosphorylation (Wang 1999). However, we were unable to abrogate *t*BOOH-induced both LPO and changes in mitochondrial $\Delta\psi$ by pre-treating hepatocytes with FK506, a specific calcineurin inhibitor (see Fig. 1). Incidentally, the lack of effect of FK506 confirms that the protective effect of CsA reported here was not due to its well-establish inhibitory effect on calcineurin phosphatase activity (Hemenway 1999), but to its capability to abrogate MPTP onset (Bernardi 1996).

Another possibility, which may well act in concert with the previous ones, is that CaMKII increases primarily mitochondrial Ca^{2+} uptake, and that the increase in mitochondrial Ca^{2+} helps *per se* to trigger MPTP opening by potentiating the capability of ROS to onset MPTP (Byrne 1999; Vercesi 2006). In line with this, a tight temporal correlation has been shown to exist between the increase in mitochondrial Ca^{2+} levels induced by *t*BOOH and the opening of MPTPs in primary cultured hepatocytes (Byrne 1999). This holds true for other cell lines as well. In permeabilized rat ventricular

myocytes, exogenously added CaM opens MPTPs in a CaMKII-dependent manner, and this effect was causally related to the uptake of Ca^{2+} released from sarcoplasmic reticulum by neighboring mitochondria (Odagiri 2009). Complementarily, CaMKII mediates increase in Ca^{2+} entry through the inner membrane of the cardiomyocytes mitochondria via the mitochondrial Ca^{2+} uniporter (Joiner 2012). Furthermore, exogenously administered CaM stimulated ROS production in the mitochondrial matrix of cardiomyocytes in part via MPTP formation (Odagiri 2009). Recent studies by another group demonstrated that mitochondrial rather than cytosolic CaMKII isoform is involved in CaM capability to open MPTPs in this cell type, since mitochondrial targeting of a CaMKII inhibitor fully abrogated this effect (Joiner 2012). However, our results in hepatocyte isolated mitochondria showing that the CaM inhibitor W7 and the CaMKII antagonist KN-62 inhibited *t*BOOH-induced MPTP formation only *partially* (see Fig. 8) suggest that cytosol-localized CaMKII cooperates with the mitochondrial one to account for the *full* mediation of this enzyme in the MPTP opening recorded in intact hepatocytes (see Fig. 1).

Another important Ca^{2+}-mediated intramitochondrial mechanism involved in *t*BOOH-mediated MPTP formation is the activation of the Ca^{2+}-dependent cysteine protease calpain. Selective inhibition of this protease was shown to *fully* abrogate *t*BOOH-induced MPTP onset in isolated rat mitochondria (Aguilar 1996); the absolute dependency of MPTP formation on calpain activity suggests that CaMKII and calpain act through a common mechanism to onset MPTP. There is some circumstantial evidence in the literature that CaMKII can phopshorylate and activate calpain, as has been shown for calpain II isolated from vascular smooth muscle (McClelland 1994). The reverse activation sequence also may occur, since calpain I, like other proteases including caspases, activates *in vitro*

autophosphorylated CaMKII by proteolysis (Rich 1990). Whether this mutual activation applies to mitochondrial calpain isoform/s remains to be ascertained. Alternatively, CaMKII-mediated phosphorylation of a protein involved in MPTP formation may sensitize this substrate for further calpain-dependent proteolysis, as was described for the calpain-induced proteolytic cleavage of GluR1 C-terminal fusion protein in cortical neurons (Yuen 2007). Irrespective of the mechanism involved, a similar common dependency on CaMKII and calpain activity to produce cell death has been identified in another apoptosis model in hepatocytes, such as that induced by the protein phosphatase inhibitor microcystin (Ding 2002). Actually, the *t*BOOH pro-apoptotic mechanisms revealed here strongly resembles those of microcystin in hepatocyes. In the case of microcystin, CaMKII is activated *before* ROS formation via inhibition of its dephosphorylation, and activated CaMKII mediates ROS mitochondrial formation via MPTP opening and further cytochrome *c* release, which triggers the execution of apoptosis (Ding 2003). Our results here showing that a similar mechanism applies for a "pure" model of OS strongly contributes to extrapolate this concept to other pro-oxidant hepatotoxicants, and to the several pathological situations involving OS as a cause of apoptotic hepatocellular death.

In summary, as schematized in Fig. 9, our study shows that the Ca^{2+}/CaM/CaMKII pathway plays a major role in *t*BOOH-induced MPTP formation, and the consequent exacerbation of both ROS formation from mitochondrial origin and hepatocellular apoptosis. This points CaM and CaMKII as promising targets for the development of new therapies to conteract hepatocellular oxidative damage.

Acknowledgments. This work was supported by grants from Agencia Nacional de Promoción Científica y Tecnológica (PICT 2010-0992), and Consejo Nacional de Investigaciones Científicas y Técnicas (PIP 112-200801-00691). We thank Justina Elena Ochoa, Diego Taborda, and Mara Ojeda for their valuable technical assistance.

Conflict of interest statement The authors declare that they have no conflict of interest

REFERENCES

Aguilar HI, Botla R, Arora AS, Bronk SF, Gores GJ (1996) Induction of the mitochondrial permeability transition by protease activity in rats: a mechanism of hepatocyte necrosis. Gastroenterology 110:558-566. doi: 10.1053/gast.1996.v110.pm8566604

Arrington DD, Van Vleet TR, Schnellmann RG (2006) Calpain 10: a mitochondrial calpain and its role in calcium-induced mitochondrial dysfunction. Am J Physiol Cell Physiol 291:C1159-C1171. doi: 10.1152/ajpcell.00207.2006

Azarashvili T, Krestinina O, Odinokova I, Evtodienko Y, Reiser G (2003) Physiological Ca^{2+} level and Ca^{2+}-induced permeability transition pore control protein phosphorylation in rat brain mitochondria. Cell Calcium 34:253-259. doi: 10.1016/S0143-4160(03)00107-6

Azzone GF, Azzi A (1965) Volume changes in liver mitochondria. Proc Natl Acad Sci USA 53:1084-1089. doi: 10.1073/pnas.53.5.1084

Baines CP, Song CX, Zheng YT, Wang GW, Zhang Jet al. (2003) Protein kinase Cepsilon interacts with and inhibits the permeability transition pore in cardiac mitochondria. Circ Res 92:873-880. doi: 10.1161/01.RES.0000069215.36389.8D

Baur H, Kasperek S, Pfaff E (1975) Criteria of viability of isolated liver cells. Hoppe Seylers Z Physiol Chem 356:827-838. doi: 10.1515/bchm2.1975.356.s1.827

Bera AK, Ghosh S (2001) Dual mode of gating of voltage-dependent anion channel as revealed by phosphorylation. J Struct Biol 135:67-72. 10.1006/jsbi.2001.4399

Bernardi P (1996) The permeability transition pore. Control points of a cyclosporin A-sensitive mitochondrial channel involved in cell death. Biochim Biophys Acta 1275:5-9. doi: 10.1016/0005-2728(96)00041-2

Berry MN, Friend DS (1969) High-yield preparation of isolated rat liver parenchymal cells: a biochemical and fine structural study. J Cell Biol 43:506-520. doi: 10.1083/jcb.43.3.506

Brnjic S, Olofsson MH, Havelka AM, Linder S (2010) Chemical biology suggests a role for calcium signaling in mediating sustained JNK activation during apoptosis. Mol Biosyst 6:767-774. doi: 10.1039/b920805d

Byrne AM, Lemasters JJ, Nieminen AL (1999) Contribution of increased mitochondrial free Ca^{2+} to the mitochondrial permeability transition induced by tert-butylhydroperoxide in rat hepatocytes. Hepatology 29:1523-1531. doi: 10.1002/hep.510290521

Chinopoulos C, dam-Vizi V (2006) Calcium, mitochondria and oxidative stress in neuronal pathology. Novel aspects of an enduring theme. FEBS J 273:433-450. doi: 10.1111/j.1742-4658.2005.05103.x

Cochrane CG (1991) Cellular injury by oxidants. Am J Med 91:23S-30S. doi: 10.1016/0002-9343(91)90280-B

Colbran RJ (2004) Targeting of calcium/calmodulin-dependent protein kinase II. Biochem J 378:1-16. doi: 10.1042/BJ20031547

Davies MJ (1989) Detection of peroxyl and alkoxyl radicals produced by reaction of hydroperoxides with rat liver microsomal fractions. Biochem J 257:603-606. doi: 10.1016/0304-4165(88)90063-3

Dimova S, Koleva M, Rangelova D, Stoythchev T (1995) Effect of nifedipine, verapamil, diltiazem and trifluoperazine on acetaminophen toxicity in mice. Arch Toxicol 70:112-118. doi: 10.1007/BF02733671

Ding WX, Nam OC (2003) Role of oxidative stress and mitochondrial changes in cyanobacteria-induced apoptosis and hepatotoxicity. FEMS Microbiol Lett 220:1-7. doi: 10.1016/S0378-1097(03)00100-9

Ding WX, Shen HM, Ong CN (2002) Calpain activation after mitochondrial permeability transition in microcystin-induced cell death in rat hepatocytes. Biochem Biophys Res Commun 291:321-331. doi: 10.1006/bbrc.2002.6453

Eguchi Y, Shimizu S, Tsujimoto Y (1997) Intracellular ATP levels determine cell death fate by apoptosis or necrosis. Cancer Res 57:1835-1840. doi: 10.1001/jama.246.19.2184.

Elrod JW, Molkentin JD (2013) Physiologic functions of cyclophilin D and the mitochondrial permeability transition pore. Circ J 77:1111-1122. doi: 10.1253/circj.CJ-13-0321

Erickson JR, Joiner ML, Guan X, Kutschke W, Yang Jet al. (2008) A dynamic pathway for calcium-independent activation of CaMKII by methionine oxidation. Cell 133:462-474. 10.1016/j.cell.2008.02.048

Fukunaga K, Yoshida M, Nakazono N (1998) A simple, rapid, highly sensitive and reproducible quantification method for plasma malondialdehyde by high-performance liquid chromatography. Biomed Chromatogr 12:300-303. doi: 10.1002/(SICI)1099-0801(199809/10)12:5<300::AID-BMC751>3.3.CO;2-R

Griffith OW (1980) Determination of glutathione and glutathione disulfide using glutathione reductase and 2-vinylpyridine. Anal Biochem 106:207-212. doi: 10.1016/0003-2697(80)90139-6. doi: 10.1016/0003-2697(80)90139-6

Grynkiewicz G, Poenie M, Tsien RY (1985) A new generation of Ca^{2+} indicators with greatly improved fluorescence properties. J Biol Chem 260:3440-3450. doi: NOT FOUND

Gschwendt M, Dieterich S, Rennecke J, Kittstein W, Mueller HJ, Johannes FJ (1996) Inhibition of protein kinase C μ by various inhibitors. Differentiation from protein kinase c isoenzymes. FEBS Lett 392:77-80. doi: 10.1016/0014-5793(96)00785-5

Hajimohammadreza I, Probert AW, Coughenour LL, Borosky SA, Marcoux FW, Boxer PA, Wang KK (1995) A specific inhibitor of calcium/calmodulin-dependent protein kinase-II provides neuroprotection against NMDA- and hypoxia/hypoglycemia-induced cell death. J Neurosci 15:4093-4101. doi: NOT FOUND

Halestrap AP, Doran E, Gillespie JP, O'Toole A (2000) Mitochondria and cell death. Biochem Soc Trans 28:170-177. doi: 10.2174/0929867033457278

Harper JF, Cheung WY, Wallace RW, Huang HL, Levine SN, Steiner AL (1980) Localization of calmodulin in rat tissues. Proc Natl Acad Sci U S A 77:366-370. doi: 10.1073/pnas.77.1.366

Hemenway CS, Heitman J (1999) Calcineurin. Structure, function, and inhibition. Cell Biochem Biophys 30:115-151. doi: 10.1007/BF02737887

Horbinski C, Chu CT (2005) Kinase signaling cascades in the mitochondrion: a matter of life or death. Free Radic Biol Med 38:2-11. doi: 10.1016/j.freeradbiomed.2004.09.030

Hudmon A, Schulman H (2002) Structure-function of the multifunctional Ca^{2+}/calmodulin-dependent protein kinase II. Biochem J 364:593-611. doi: 10.1042/BJ20020228

Imberti R, Nieminen AL, Herman B, Lemasters JJ (1993) Mitochondrial and glycolytic dysfunction in lethal injury to hepatocytes by t-butylhydroperoxide: protection by fructose, cyclosporin A and trifluoperazine. J Pharmacol Exp Ther 265:392-400. doi: NOT FOUND

Itano T, Matsui H, Doi A, Ohmura Y, Hatase O (1986) Identification of calmodulin-binding proteins in pure mitochondria by photoaffinity labeling. Biochem Int 13:787-792. doi: NOT FOUND

Jeong SY, Seol DW (2008) The role of mitochondria in apoptosis. BMB Rep 41:11-22. doi: 10.5483/BMBRep.2008.41.1.011

Joiner ML, Koval OM, Li J, He BJ, Allamargot Cet al. (2012) CaMKII determines mitochondrial stress responses in heart. Nature 491:269-273. doi: 10.1038/nature11444

Kanno T, Sato EE, Muranaka S, Fujita H, Fujiwara T, Utsumi T, Inoue M, Utsumi K (2004) Oxidative stress underlies the mechanism for Ca^{2+}-induced permeability transition of mitochondria. Free Radic Res 38:27-35. doi: 10.1080/10715760310001626266

Kim BJ, Ryu SW, Song BJ (2006) JNK- and p38 kinase-mediated phosphorylation of Bax leads to its activation and mitochondrial translocation and to apoptosis of human hepatoma HepG2 cells. J Biol Chem 281:21256-21265. doi: 10.1074/jbc.M510644200

Korsmeyer SJ, Wei MC, Saito M, Weiler S, Oh KJ, Schlesinger PH (2000) Pro-apoptotic cascade activates BID, which oligomerizes BAK or BAX into pores that result in the release of cytochrome c. Cell Death Differ 7:1166-1173. doi: 10.1038/sj.cdd.4400783

Kuroda S, Nakai A, Kristian T, Siesjo BK (1997) The calmodulin antagonist trifluoperazine in transient focal brain ischemia in rats. Anti-ischemic effect and therapeutic window. Stroke 28:2539-2544. doi: 10.1161/01.STR.28.12.2539

Lee CS, Park SY, Ko HH, Song JH, Shin YK, Han ES (2005) Inhibition of MPP+-induced mitochondrial damage and cell death by trifluoperazine and W-7 in PC12 cells. Neurochem Int 46:169-178. doi: 10.1016/j.neuint.2004.07.007

Lee KK, Shimoji M, Hossain QS, Sunakawa H, Aniya Y (2008) Novel function of glutathione transferase in rat liver mitochondrial membrane: role for cytochrome c release from mitochondria. Toxicol Appl Pharmacol 232:109-118. doi: 10.1016/j.taap.2008.06.005

Lemasters JJ, Theruvath TP, Zhong Z, Nieminen AL (2009) Mitochondrial calcium and the permeability transition in cell death. Biochim Biophys Acta 1787:1395-1401. doi: 10.1016/j.bbabio.2009.06.009

Li J, Wang P, Yu S, Zheng Z, Xu X (2012) Calcium entry mediates hyperglycemia-induced apoptosis through Ca^{2+}/calmodulin-dependent kinase II in retinal capillary endothelial cells. Mol Vis 18:2371-2379. doi: NOT FOUND

Liu G, Zhao J, Chang Z, Guo G (2013) CaMKII activates ASK1 to induce apoptosis of spinal astrocytes under oxygen-glucose deprivation. Cell Mol Neurobiol 33:543-549. doi: 10.1007/s10571-013-9920-0

Liu Y, Templeton DM (2007) Cadmium activates CaMK-II and initiates CaMK-II-dependent apoptosis in mesangial cells. FEBS Lett 581:1481-1486. doi: 0.1016/j.febslet.2007.03.003

Lowry OH, Rosebrough NJ, Farr AL, Randall RJ (1951) Protein measurement with the Folin phenol reagent. J Biol Chem 193:265-275. doi: NOT FOUND

Lyman GE, DeVincenzo JP (1967) Determination of picogram amounts of ATP using the luciferin-luciferase enzyme system. Anal Biochem 21:435-443. doi: 10.1016/0003-2697(67)90318-1

Majumder PK, Mishra NC, Sun X, Bharti A, Kharbanda S, Saxena S, Kufe D (2001) Targeting of protein kinase C delta to mitochondria in the oxidative stress response. Cell Growth Differ 12:465-470. doi: NOT FOUND

McClelland P, Adam LP, Hathaway DR (1994) Identification of a latent Ca2+/calmodulin dependent protein kinase II phosphorylation site in vascular calpain II. J Biochem 115:41-46. doi: NOT FOUND

Molkentin JD (2001) Calcineurin, mitochondrial membrane potential, and cardiomyocyte apoptosis. Circ Res 88:1220-1222. doi: NOT FOUND

Muriel P (2009) Role of free radicals in liver diseases. Hepatol Int 3:526-536. doi: 10.1007/s12072-009-9158-6

Nguyen A, Chen P, Cai H (2004) Role of CaMKII in hydrogen peroxide activation of ERK1/2, p38 MAPK, HSP27 and actin reorganization in endothelial cells. FEBS Lett 572:307-313. doi: 10.1016/j.febslet.2004.06.061

Nieminen AL, Byrne AM, Herman B, Lemasters JJ (1997) Mitochondrial permeability transition in hepatocytes induced by t-BuOOH: NAD(P)H and reactive oxygen species. Am J Physiol 272:C1286-C1294. doi: NOT FOUND

Nieminen AL, Saylor AK, Tesfai SA, Herman B, Lemasters JJ (1995) Contribution of the mitochondrial permeability transition to lethal injury after exposure of hepatocytes to t-butylhydroperoxide. Biochem J 307 (Pt 1):99-106. doi: 10.1016/0270-9139(93)92139-Q

Odagiri K, Katoh H, Kawashima H, Tanaka T, Ohtani H, Saotome M, Urushida T, Satoh H, Hayashi H (2009) Local control of mitochondrial membrane potential, permeability transition pore and reactive oxygen species by calcium and calmodulin in rat ventricular myocytes. J Mol Cell Cardiol 46:989-997. doi: 10.1016/j.yjmcc.2008.12.022

Orrenius S, Burkitt MJ, Kass GE, Dypbukt JM, Nicotera P (1992) Calcium ions and oxidative cell injury. Ann Neurol 32 Suppl:S33-S42. doi: 10.1002/ana.410320708

Orrenius S, Gogvadze V, Zhivotovsky B (2007) Mitochondrial oxidative stress: implications for cell death. Annu Rev Pharmacol Toxicol 47:143-183. doi: 10.1146/annurev.pharmtox.47.120505.105122

Perez LM, Milkiewicz P, Ahmed-Choudhury J, Elias E, Ochoa JE, Sanchez Pozzi EJ, Coleman R, Roma MG (2006) Oxidative stress induces actin-cytoskeletal and tight-junctional alterations in hepatocytes by a Ca^{2+} -dependent, PKC-mediated mechanism: protective effect of PKA. Free Radic Biol Med 40:2005-2017. doi: 10.1016/j.freeradbiomed.2006.01.034

Rich DP, Schworer CM, Colbran RJ, Soderling TR (1990) Proteolytic activation of calcium/calmodulin-dependent protein kinase II: Putative function in synaptic plasticity. Mol Cell Neurosci 1:107-116. doi: NOT FOUND

Ronco MT, Alvarez ML, Monti JA, Carrillo MC, Pisani GB, Lugano MC, Carnovale CE (2004) Role of nitric oxide increase on induced programmed cell death during early stages of rat liver regeneration. Biochim Biophys Acta 1690:70-76. doi: 10.1016/j.bbadis.2004.05.004

Roy DN, Mandal S, Sen G, Biswas T (2009) Superoxide anion mediated mitochondrial dysfunction leads to hepatocyte apoptosis preferentially in the periportal region during copper toxicity in rats. Chem Biol Interact 182:136-147. doi: 10.1016/j.cbi.2009.08.014

Ruvolo PP, Deng X, Carr BK, May WS (1998) A functional role for mitochondrial protein kinase Cα in Bcl2 phosphorylation and suppression of apoptosis. J Biol Chem 273:25436-25442. doi: 10.1074/jbc.273.39.25436

Scaduto RC, Jr., Grotyohann LW (1999) Measurement of mitochondrial membrane potential using fluorescent rhodamine derivatives. Biophys J 76:469-477. doi: 10.1016/S0006-3495(99)77214-0

Schwertz H, Carter JM, Abdudureheman M, Russ M, Buerke Uet al. (2007) Myocardial ischemia/reperfusion causes VDAC phosphorylation which is reduced by cardioprotection with a p38 MAP kinase inhibitor. Proteomics 7:4579-4588. doi: 10.1002/pmic.200700734

Takano H, Fukushi H, Morishima Y, Shirasaki Y (2003) Calmodulin and calmodulin-dependent kinase II mediate neuronal cell death induced by depolarization. Brain Res 962:41-47. doi: 10.1016/S0006-8993(02)03932-X

Takeyama N, Matsuo N, Tanaka T (1993) Oxidative damage to mitochondria is mediated by the Ca^{2+}-dependent inner-membrane permeability transition. Biochem J 294 (Pt 3):719-725. doi: NOT FOUND

Thor H, Hartzell P, Orrenius S (1984) Potentiation of oxidative cell injury in hepatocytes which have accumulated Ca^{2+}. J Biol Chem 259:6612-6615. doi: NOT FOUND

Tietze F (1969) Enzymic method for quantitative determination of nanogram amounts of total and oxidized glutathione: applications to mammalian blood and other tissues. Anal Biochem 27:502-522. doi: 10.1016/0003-2697(69)90064-5

Timmins JM, Ozcan L, Seimon TA, Li G, Malagelada Cet al. (2009) Calcium/calmodulin-dependent protein kinase II links ER stress with Fas and mitochondrial apoptosis pathways. J Clin Invest 119:2925-2941. doi: 10.1172/JCI38857

Tsuruta F, Sunayama J, Mori Y, Hattori S, Shimizu S, Tsujimoto Y, Yoshioka K, Masuyama N, Gotoh Y (2004) JNK promotes Bax translocation to mitochondria through phosphorylation of 14-3-3 proteins. EMBO J 23:1889-1899. doi: 10.1038/sj.emboj.7600194

Tzung SP, Fausto N, Hockenbery DM (1997) Expression of Bcl-2 family during liver regeneration and identification of Bcl-x as a delayed early response gene. Am J Pathol 150:1985-1995. doi: NOT FOUND

Vercesi AE, Kowaltowski AJ, Oliveira HC, Castilho RF (2006) Mitochondrial Ca^{2+} transport, permeability transition and oxidative stress in cell death: implications in cardiotoxicity, neurodegeneration and dyslipidemias. Front Biosci 11:2554-2564. doi: 10.2741/1990

Vermes I, Haanen C, Steffens-Nakken H, Reutelingsperger C (1995) A novel assay for apoptosis. Flow cytometric detection of phosphatidylserine expression on early apoptotic cells using fluorescein labelled Annexin V. J Immunol Methods 184:39-51. doi: 10.1016/0022-1759(95)00072-I

Villarruel MC, Fernandez G, de Ferreyra EC, de Fenos OM, Castro JA (1990) Modulation of the course of CCl_4-induced liver injury by the anti-calmodulin drug thioridazine. Toxicol Lett 51:13-21. doi: NOT FOUND

Wang HG, Pathan N, Ethell IM, Krajewski S, Yamaguchi Yet al. (1999) Ca^{2+}-induced apoptosis through calcineurin dephosphorylation of BAD. Science 284:339-343. doi: 10.1126/science.284.5412.339

Yaglom JA, Ekhterae D, Gabai VL, Sherman MY (2003) Regulation of necrosis of H9c2 myogenic cells upon transient energy deprivation. Rapid deenergization of mitochondria precedes necrosis and is controlled by reactive oxygen species, stress kinase JNK, HSP72 and ARC. J Biol Chem 278:50483-50496. doi: 10.1074/jbc.M306903200

Yuen EY, Liu W, Yan Z (2007) The phosphorylation state of GluR1 subunits determines the susceptibility of AMPA receptors to calpain cleavage. J Biol Chem 282:16434-16440. doi: 10.1074/jbc.M701283200

Table-1

Effect of tBOOH on cellular integrity, redox status and Ca^{2+} levels

	DMSO [a]	*t*BOOH[b]
Cellular viability (% of total cells)	96 ± 3	62 ± 3*
LDH release (% of total cell content)	32 ± 2	42 ± 3*
ATP cellular content (µmol/10^6 cells)	48 ± 6	43 ± 3
MDA cellular content /nmol/mg prot.)	1.3 ± 0,2	8,0 ± 0,3*
Total glutathione (mg/mg of protein)	27 ± 2	17 ± 1*
GSSG-to-total glutathione ratio (%)	3,1 ± 0,1	4,1 ± 0,2*
Cytosolic free Ca^{2+} (nM)	119 ± 11	3029 ± 474*

Cells were pretreated for 15 min either with *t*BOOH (500 µM) or DMSO (controls).

Note: LDH, lactate dehydrogenase; ATP, adenosine triphosphate; MDA, malondialdehyde; GSSG, oxidized glutathione.

* $p < 0.05$ vs. DMSO, for $n = 4$-10.

FIGURE LEGENDS

Figure 1. *Involvement of Ca^{2+} and signalling molecules acting downstream of Ca^{2+} in tBOOH-induced mitochondrial permeability transition (MPT), and the subsequent* malondialdehyde *(MDA) formation.* (*A*) Effect of the intracellular Ca^{2+} chelator BAPTA/AM (50 µM), the antagonists of CaM trifluoperazine (TFP, 10 µM) and W7 (100 µM; with or without 5 µM cyclosporin A-CsA), the calcineurin inhibitor FK-506 (1 µM), or the CaMKII inhibitor KN-62 (10 µM) on *t*BOOH (500 µM, 15 min)-induced MPT, as assessed by measuring mitochondrial membrane depolarization as a surrogate marker, using tetra-methyl-rhodamine methyl ester as a fluorescent probe. Mitochondrial membrane depolarization was expressed as the percentage of the change in mitochondrial depolarization, in a scale ranging from a basal, non-depolarized condition (control value) to the maximal depolarized condition, obtained by adding the respiratory chain uncoupling compound, carbonyl cyanide m-chloro-phenylhydrazone (10 µM). The dotted line represents the mean value of the change in mitochondrial $\Delta\psi$ induced by *t*BOOH in hepatocytes pretreated with the MPTP blocker CsA (54 ± 3%); the differences of the values of the different experimental groups with this reference value reflects MPT-dependent changes in mitochondrial $\Delta\psi$. (*B*) Effect of these pre-treatments on *t*BOOH-induced LPO, as evaluated by measuring MDA formation. The dotted line represents the mean value of the MDA content in CsA-pretreated hepatocytes exposed to *t*BOOH (54 ± 3%); the differences of the values of the different experimental groups with this reference value reflects MPT-dependent MDA formation.

Note that BAPTA, the CaM antagonists and the CaMKII inhibitor prevented partially both MPTP and MDA formation to the same extent as the MPT blocker CsA did, suggesting that

MPTP formation and the subsequent LPO are facilitated by Ca^{+2} elevations, and this phenomena are modulated by CaM via CaMKII activation. Contrarily, the calcineurin inhibitor FK-506 was without effect, suggesting that calcineurin play no role in *t*BOOH effects.

Values are mean ± SE, for 4-10 independent experiments. [a]Significantly different from control ($p < 0 .05$); [b]significantly different from *t*BOOH-treated cells ($p < 0.05$).

Figure 2. *Activation by phosphorylation of CaMKII by tBOOH, and its prevention by CaM and CaMKII inhibition. Upper panel:* Representative Western blottings of phospho (p)-CaMKII and total CaMKII content in whole cellular lysates of cultured rat hepatocytes, exposed to *t*BOOH (500 µM, 15 min), with or without a 15-min pre-treatment with the CaM antagonists trifluorperazine (TFP, 10 µM) and W7 (100 µM), or with the CaMKII inhibitor KN-62 (10 µM). *Lower panel:* CaMKII phosphorylation status for each experimental condition, expressed as the phosphorylated-to-total CaMKII ratio, and referred to control values. Results are mean ± SE, for 5 independent experiments. [a]Significantly different from control ($p < 0.05$); [b]significantly different from *t*BOOH-treated cells ($p < 0.05$).

Figure 3. *Activation by phosphorylation of JNK1/2 and p38^{MAPK} by tBOOH, and its prevention by intracellular Ca^{2+} chelation and CaM/CaMKII inhibition. Upper panels:* Representative Western blottings of (*A*) phospho (p)-JNK1/2 and (*B*) p-p38 MAPK, and of the total content of these MAPK in whole lysates of cultured rat hepatocytes, exposed to *t*BOOH (500 µM, 15 min), with or without a 15-min pre-treatment with the Ca^{2+} chelating

agent BAPTA/AM (50 μM), the CaM antagonists trifluorperazine (TFP, 10 μM) and W7 (100 μM), or the CaMKII inhibitor KN-62 (10 μM). *Lower panels:* JNK1/2 and p38^{MAPK} phosphorylation status for each experimental condition, expressed as the phosphorylated-to-total ratio, and referred to control values. Results are mean ± SE, for 4 independent experiments. [a]Significantly different from control ($p < 0$ .05); [b]significantly different from *t*BOOH-treated cells ($p < 0.05$).

Figure 4. *Involvement of the Ca2+/CaM/CaMKII signaling pathway in tBOOH-induced apoptosis.* Apoptosis was assessed with annexin V-FITC and propidium iodide (PI) staining, by using flow cytometry analysis. Cells in culture were incubated with *t*BOOH (500 μM, 15 min), with or without a 15-min pre-treatment with the mitochondrial permeability transtion blocker cyclosporin A (CsA, 5 μM), the intracellular Ca^{2+} chelator BAPTA/AM (50 μM), the CaM antagonists trifluorperazine (TFP, 10 μM) and W7 (100 μM), or the CaMKII inhibitor KN-62 (10 μM). The percentages of cells (referred to control values) with early apoptosis [annexin V (+)/PI (-)], with late apoptosis [annexin V (+)/PI (+)], or with any stage of apoptosis [annexin V (+)], are depicted in the panels *A*, *B*, and *C*, respectively. Results represent mean ± SEM of 3 experiments. [a]Significantly different from control ($p < 0$ .05); [b]significantly different from *t*BOOH-treated cells ($p < 0.05$).

Figure 5. *Involvement of the Ca2+/CaM/CaMKII signaling pathway in tBOOH-induced mitochondrial release of cytochrome c. Upper panel:* Representative Western blottings of cytochrome *c* content in the cytosolic fraction of cultured rat hepatocytes exposed to *t*BOOH (500 μM, 15 min), with or without a 15-min pre-treatment with the CaM antagonist

W7 (100 µM), or with the CaMKII inhibitor KN-62 (10 µM); ß-actin was used as loading control. *Lower panel:* Densitometric analysis of cytochrome *c* electrophorectic bands for each experimental condition, referred to the respective signal intensity of ß-actin, and expressed as percentage of control values. Data are mean ± SE for 5 separate experiments. [a]Significantly different from control ($p < 0$ .05); [b]significantly different from *t*BOOH-treated cells ($p < 0.05$).

Figure 6. *Involvement of the Ca2+/CaM/CaMKII signaling pathway in tBOOH-induced activation of caspase-3*. Activity of caspase-3 in cultured cells exposed to *t*BOOH (500 µM, 15 min), with or without a 15-min pre-treatment with the mitochondrial permeability transtion blocker cyclosporin A (CsA, 5 µM), the intracellular Ca^{2+} chelator BAPTA/AM (50 µM), the CaM antagonists trifluorperazine (TFP, 10 µM) and W7 (100 µM), or the CaMKII inhibitor KN-62 (10 µM). Caspase-3 activity was determined by using a fluorometric assay, as described in *Material and Methods* Section. Bars represent activity expressed as percentage of control values. Data are mean ± SE for 4 independent experiments. [a]Significantly different from control group ($p < 0$ .05); [b]significantly different from *t*BOOH-treated cells ($p < 0.05$).

Figure 7. *Involvement of the Ca2+/CaM/CaMKII signaling pathway in tBOOH-induced increase in the Bax-to-Bcl-xL ratio*. *Upper panel:* Representative Western blottings of Bax and Bcl-xL illustrating their protein expressions in the mitochondrial fraction of cultured rat hepatocytes exposed to *t*BOOH (500 µM, 15 min), with or without a 15-min pre-treatment with the CaM antagonist W7 (100 µM), or the CaMKII inhibitor KN-62 (10 µM);

prohibitin was used as a mitochondrial protein loading control. *Lower panel:* Bax-to-Bcl-xL ratio for each experimental condition, calculated from the densitometric analysis of the electrophorectic bands of these proteins normalized to the respective signal intensity of prohibitin, and expressed as percentage of controls. Data are mean ± SE for 3 independent experiments. [a]Significantly different from control group ($p < 0.05$); [b]significantly different from *t*BOOH-treated cells ($p < 0.05$).

Figure 8. *Effect of CaM and CaMKII antagonists on tBOOH-induced swelling of isolated rat liver mitochondria.* Mitochondria were suspended at a concentration of 0.5 mg of protein/ml, and a 2-min baseline of light scattering at 540 nm was obtained. Then, *t*BOOH (500 μM final concentration) was added to the swelling buffer, together (or not) with the mitochondrial permeability transtion blocker cyclosporin A (CsA, 5 μM), the CaM antagonist W7 (100 μM), or the CaMKII inhibitor KN-62 (10 μM). Changes in light scattering at 540 nm were then recorded at 30-s intervals for 15 min. Data are mean ± SE for 8-16 independent experiments. *$p < 0.005$; [#]$p < 0.001$.

Figure 9. *Schematic representation of the main conslusions drawn from this study.* The Ca^{2+}-calmodulin (CaM)-dependent protein kinase type II (CaMKII) signaling pathway mediates the facilitating role of oxidative-stress-induced Ca^{2+} mitochondrial permeability transition via both the onset of the mitochondrial permeability transition pore (MPTP), probably via $p38^{MAPK}$ (p38) activation, and Bax translocation to mitochondria, probably via JNK activation. Disruption of the mitochondrial permeability barrier leads to: *a)* impairment of the mitochondrial electron transport chain with leakage of electrons and

subsequent ROS generation from mitochondrial origin, which contributes to the amplification/perpetuation of the oxidative damage, and *b)* hepatocellular death by apoptosis via the mitochondrial pathway, due to the mitochondrial pore-mediated release of cytochrome *c* (Cyt *c*), followed by apoptosome formation and activation of caspase-3 (Casp-3).

Figure 1
Click here to download high resolution image

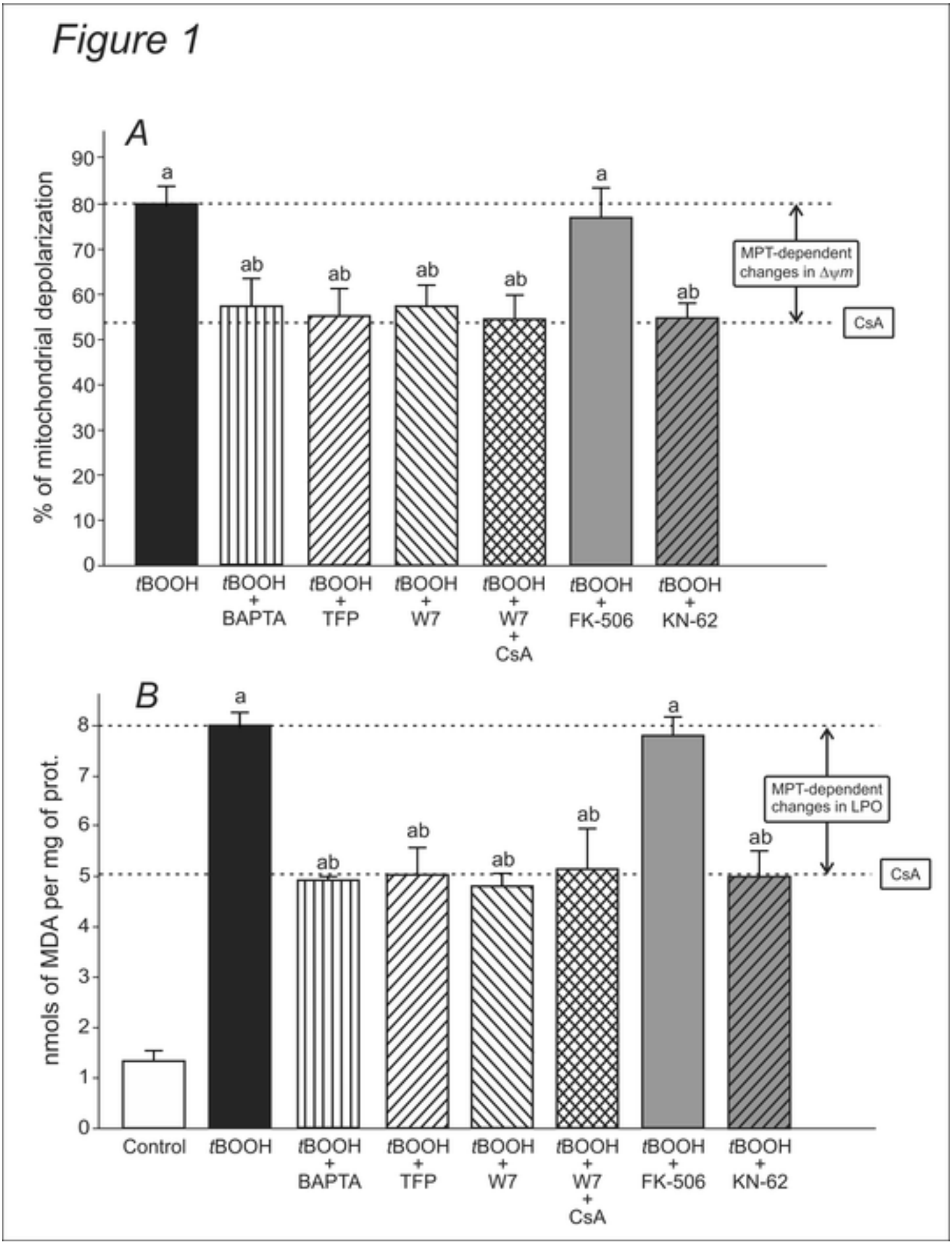

Figure 2
Click here to download high resolution image

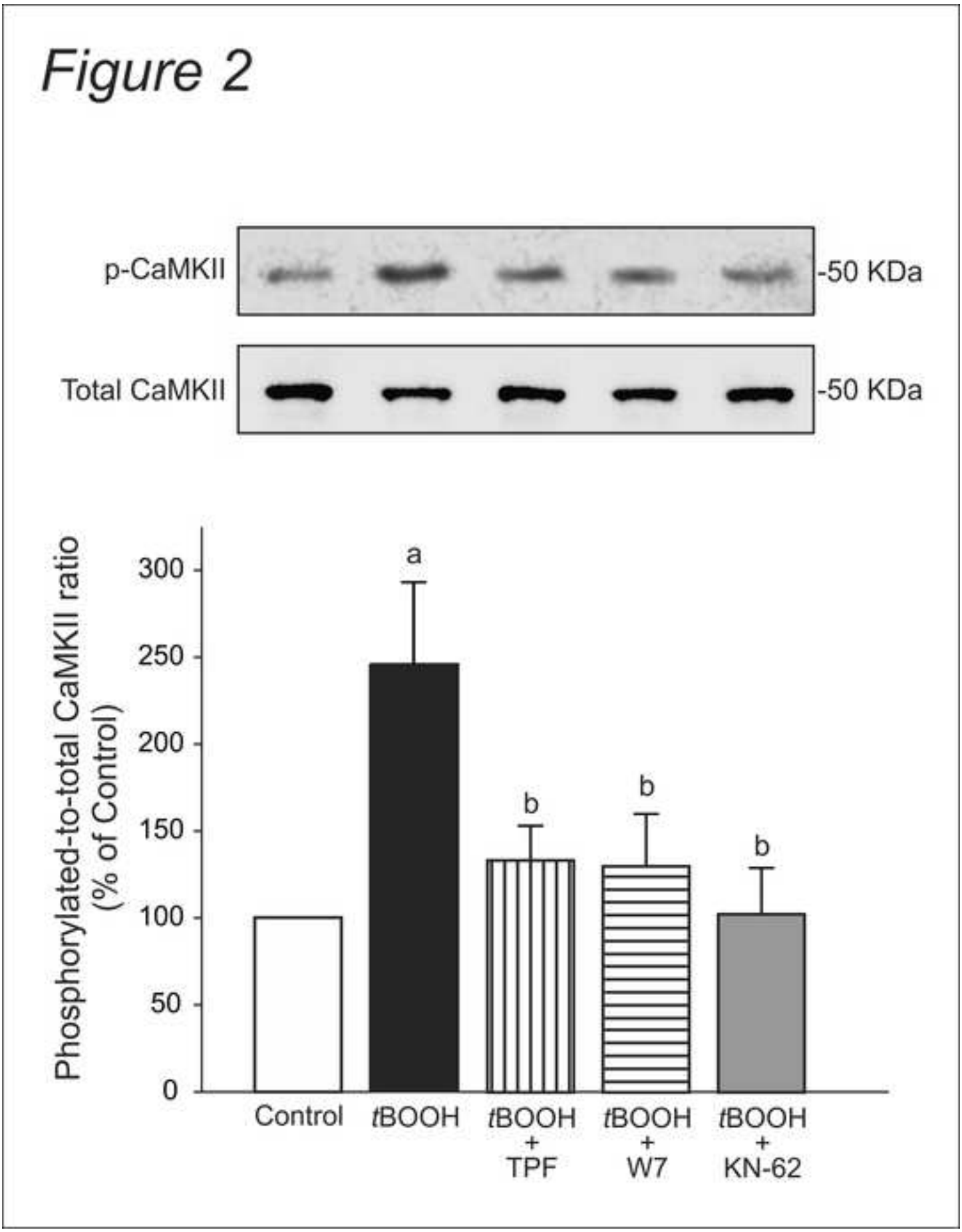

Figure 3

Click here to download high resolution image

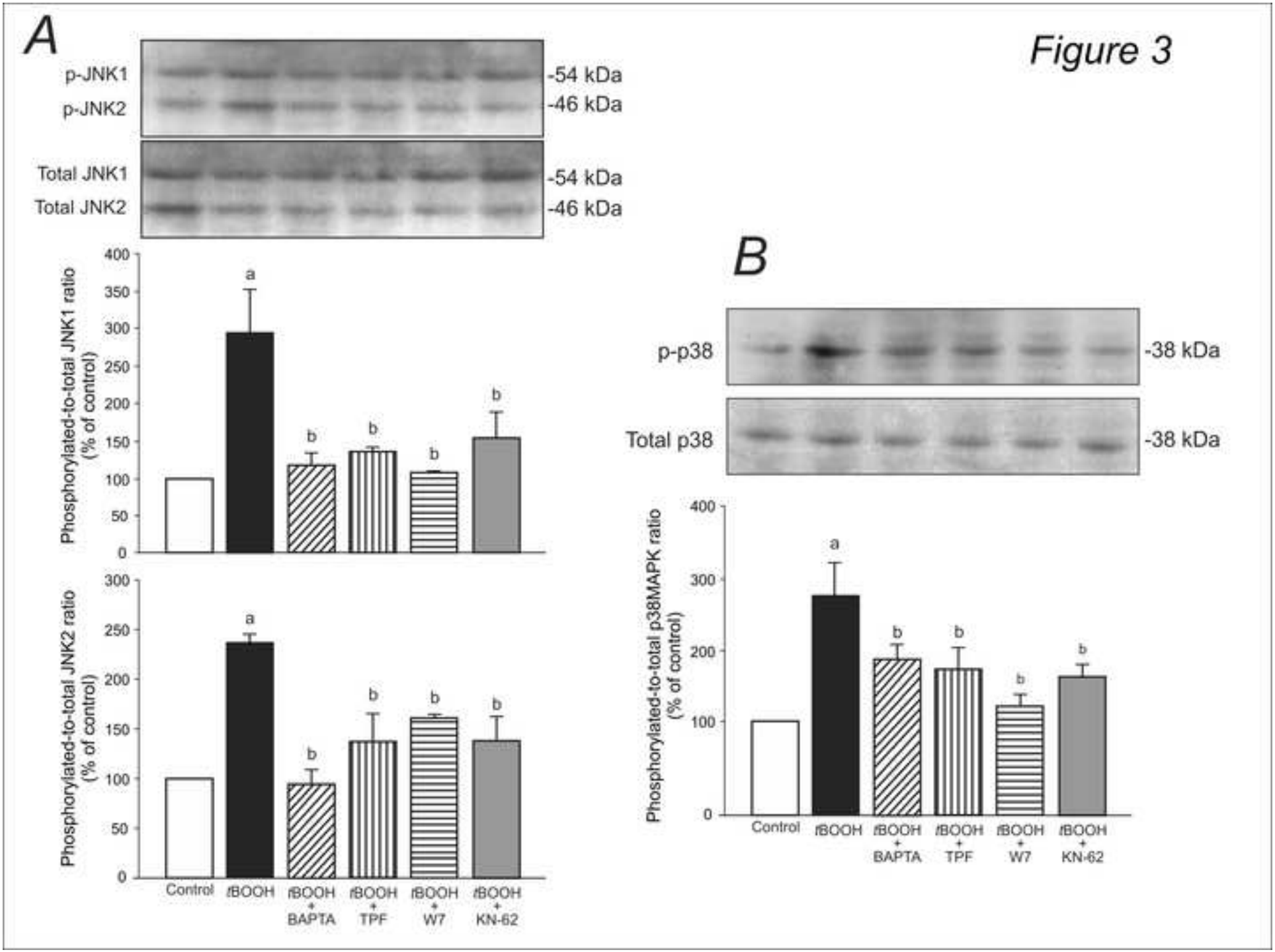

Figure 4
Click here to download high resolution image

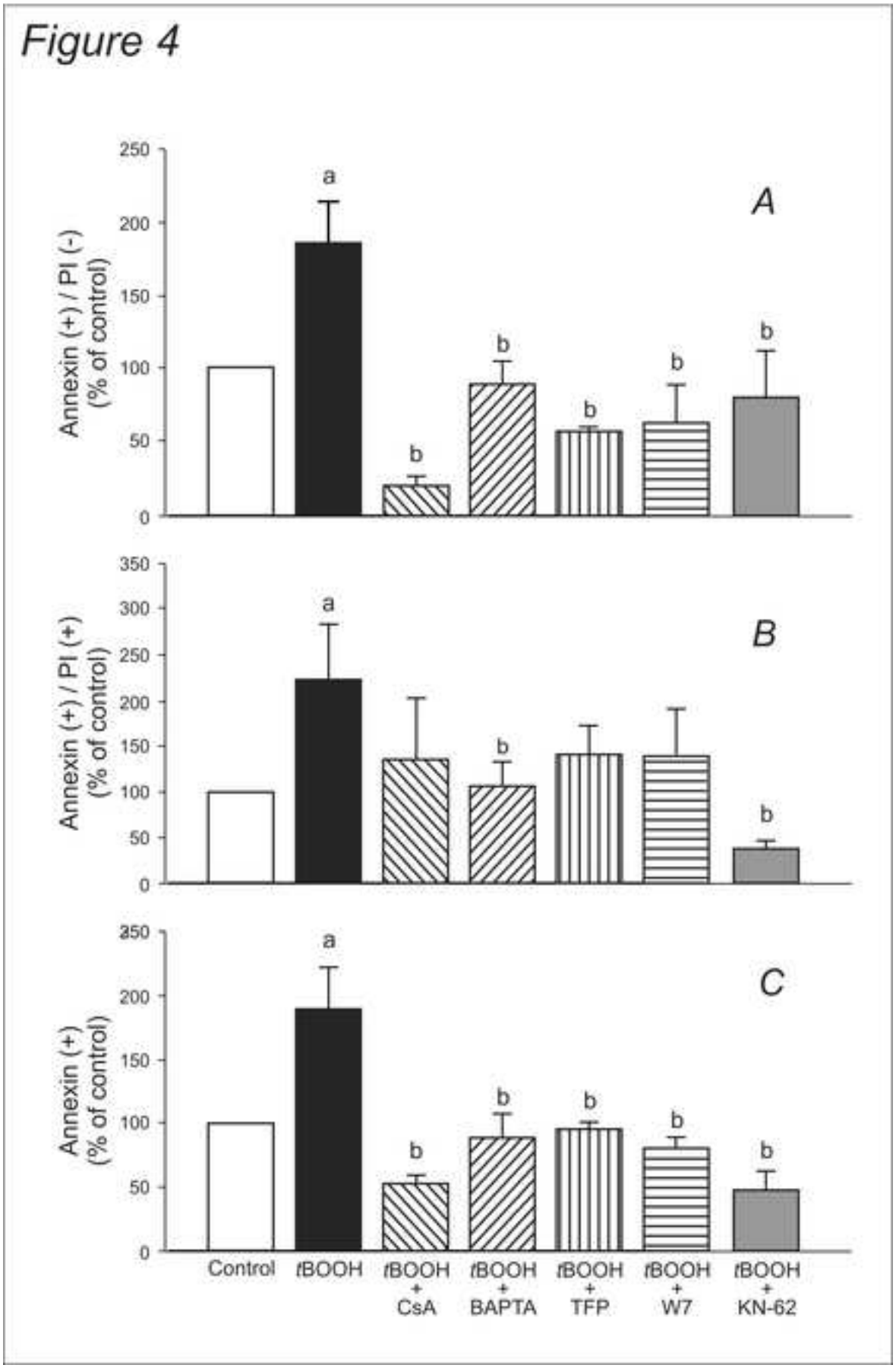

Figure 5
Click here to download high resolution image

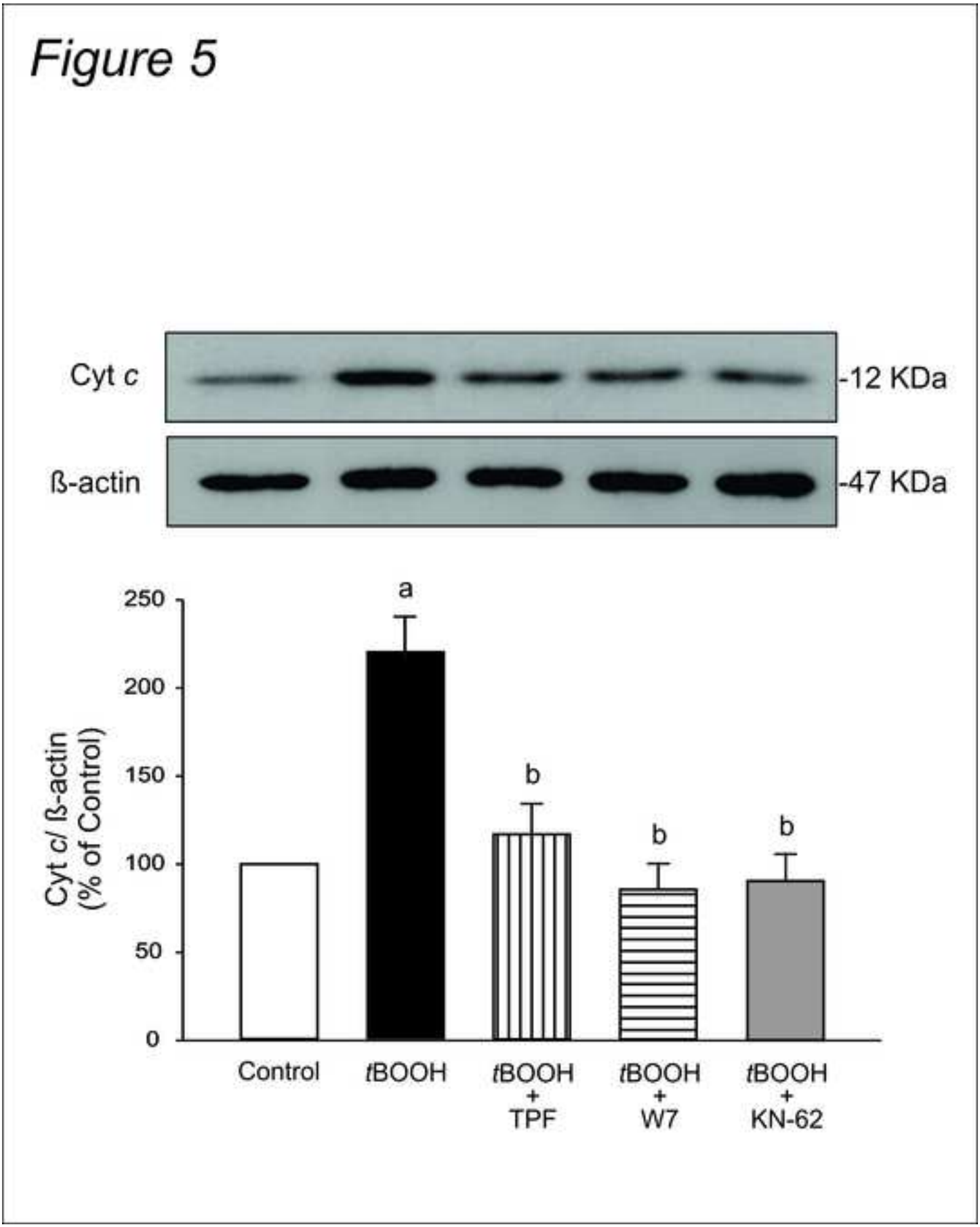

Figure 6
Click here to download high resolution image

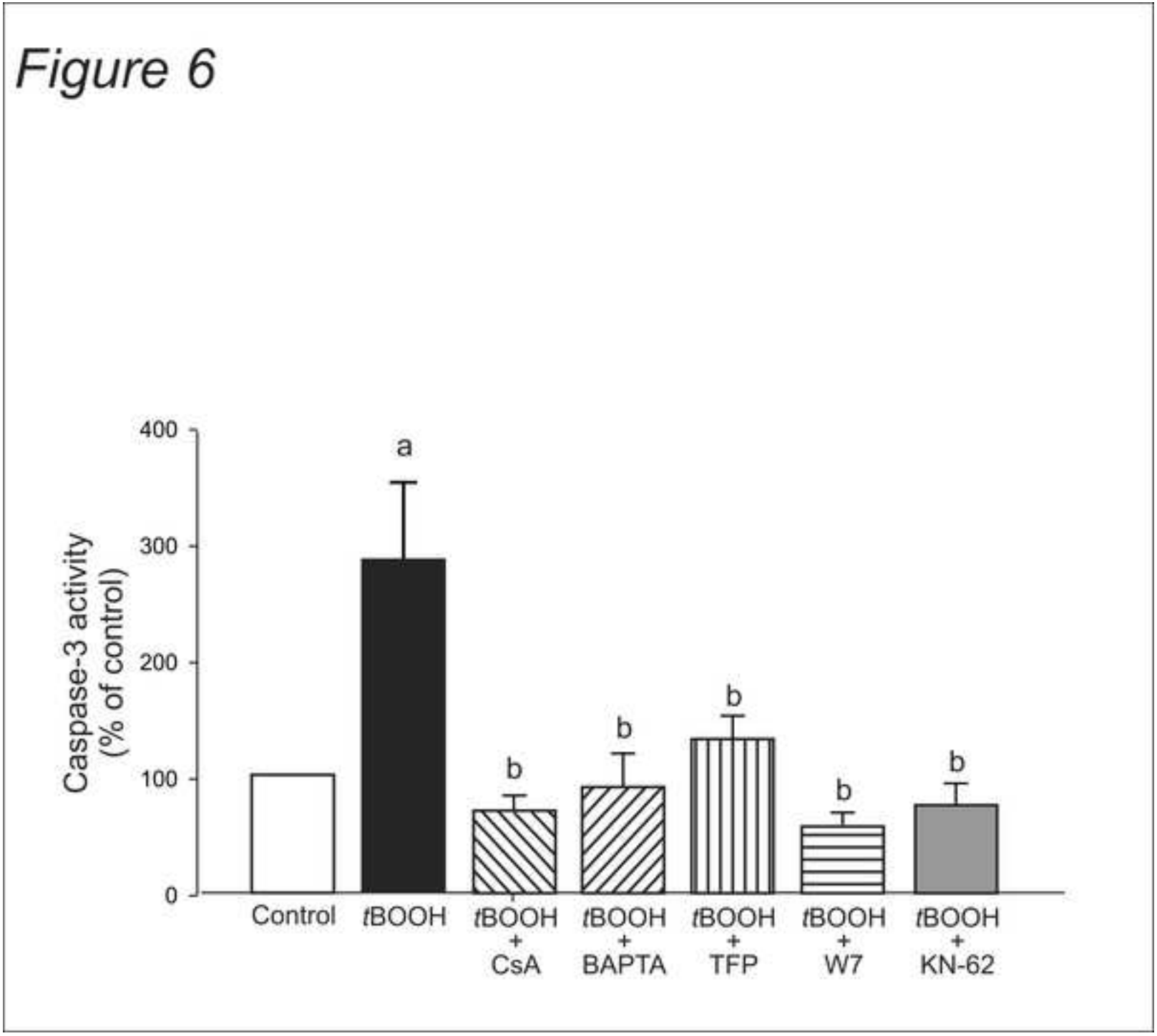

Figure 7
Click here to download high resolution image

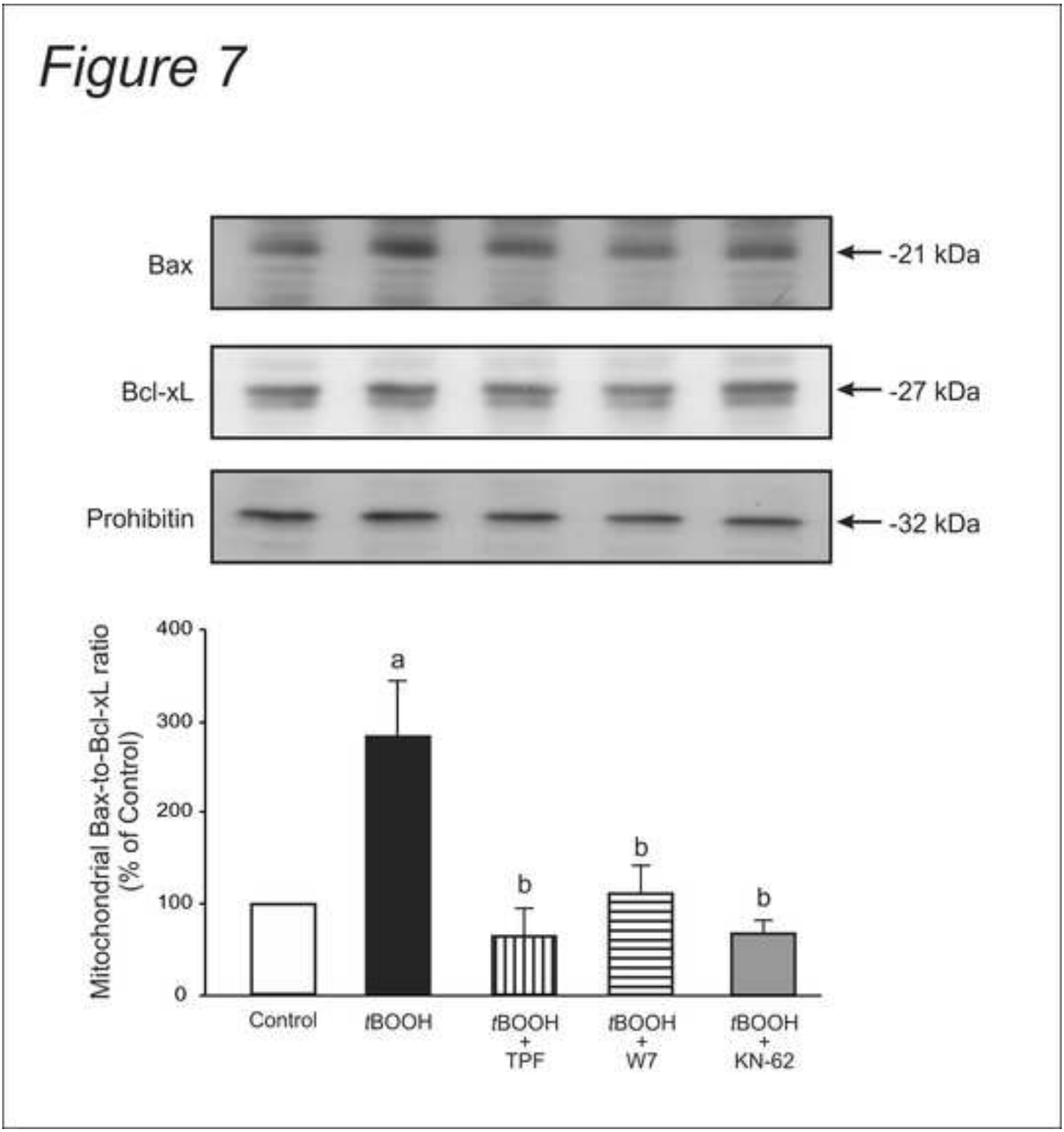

Figure 8

Click here to download high resolution image

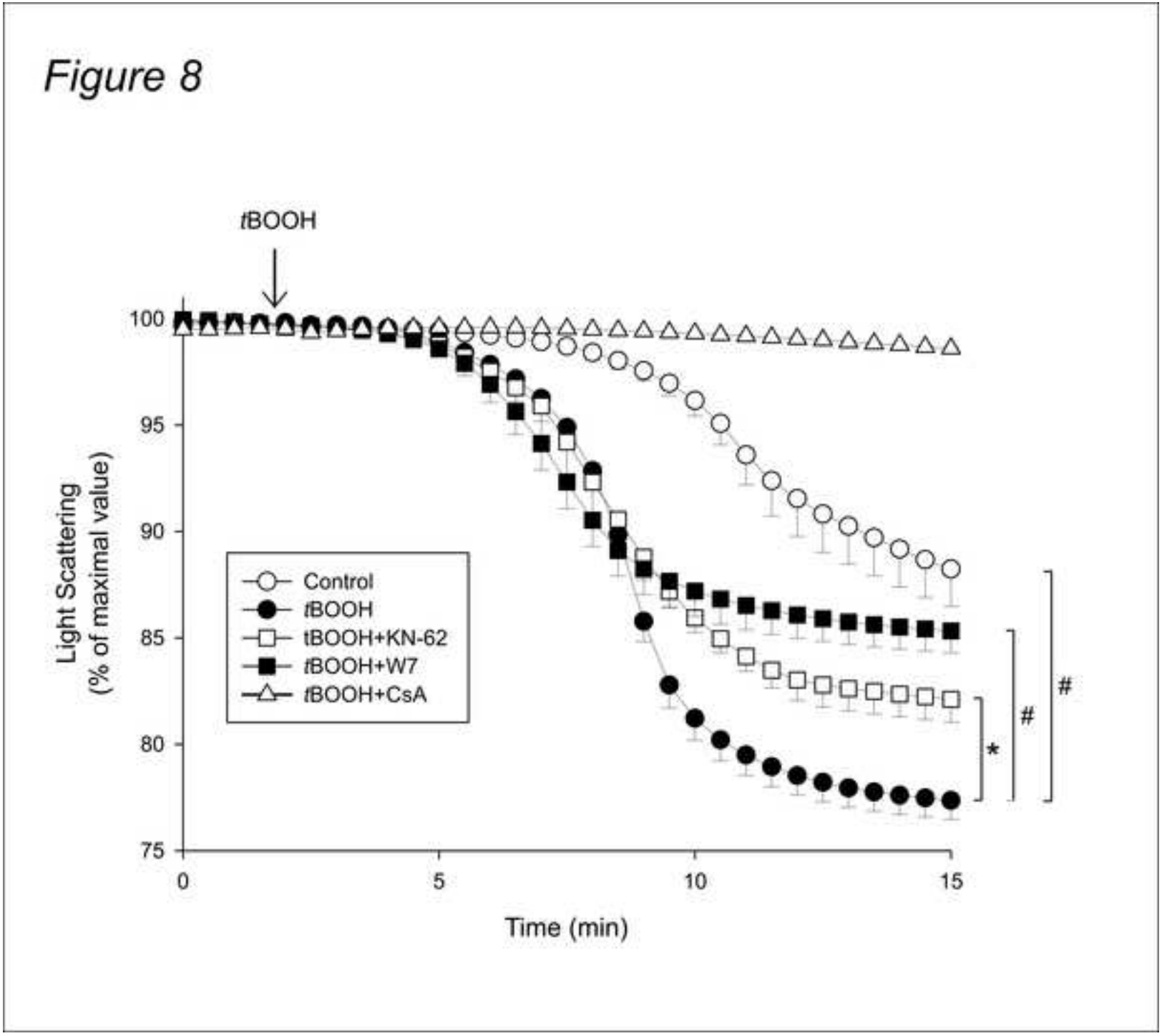

Figure 9
Click here to download high resolution image